UCLA
COMPUTATIONAL AND APPLIED MATHEMATICS

Resistive Instabilities in Rapidly Rotating Fluids: Linear Theory of the Convective Modes

Weijia Kuang
Paul H. Roberts

December 1991

CAM Report 91-28

Department of Mathematics
University of California, Los Angeles
Los Angeles, CA. 90024-1555

RESISTIVE INSTABILITIES IN RAPIDLY ROTATING FLUIDS: LINEAR THEORY OF THE CONVECTIVE MODES

WEIJIA KUANG and PAUL H. ROBERTS
Department of Mathematics, University of California, Los Angeles, California, CA 90024

This paper analyzes the linear stability of a rapidly-rotating, stratified sheet pinch in a gravitational field, $\mathbf{g}$, perpendicular to the sheet. The sheet pinch is a layer ($0 \leq z \leq d$) of inviscid, Boussinesq fluid of electrical conductivity σ, magnetic permeability μ, and almost uniform density ρ_0; z is height. The prevailing magnetic field, $\mathbf{B}_0(z)$, is horizontal at each z level, but varies in direction with z. The angular velocity, $\mathbf{\Omega}$ is vertical and large ($\Omega \gg V_A/d$, where $V_A = B_0/\sqrt{(\mu\rho_0)}$ is the Alfvén velocity). The Elsasser number, $\Lambda = \sigma B_0^2/2\Omega\rho_0$, measures σ. A (modified) Rayleigh number, $R = g\beta d^2/\rho_0 V_A^2$, measures the buoyancy force, where $\boldsymbol{\beta}$ is the imposed density gradient, antiparallel to $\mathbf{g}$. A Prandtl number, $p_\kappa = \mu\sigma\kappa$, measures the diffusivity, κ, of density differences.

The case $R = 0$ was studied in Part 1 of this series. It was shown that "resistive instabilities", known as "tearing modes", exist when Λ is large enough, when the horizontal wavenumber, k, of the instability is small enough, and when at least one "critical level" exists within the layer, i.e. a value of z at which $\mathbf{B}$ is perpendicular to the horizontal wavevector, $\mathbf{k}$. In Part 2, gravitational modes ("g–modes") were studied under the assumption of zero density diffusion ($p_\kappa = 0$). Instability occurs for any $\mathbf{k}$ provided R is sufficiently large; critical layers need not exist; k need not be small. The growth rate of the most rapidly growing disturbance, the "fast g–mode" for $kd = O(\Lambda^{1/2})$, is independent of σ. The structure of "g–modes" is quite different from that of tearing modes; e.g., when a single critical layer is centrally placed, the velocity disturbance is almost symmetric about it but for the tearing modes it is nearly antisymmetric. In conditions in which tearing is possible for $R = 0$, the marginal g–mode require a top-heavy density distribution to stabilize it ($R_m < 0$), and is overstable.

It is shown here that, when $p_\kappa \neq 0$, the stability characteristics are very different. Again, the layer can be stabilized in the tearing range only by a negative R, but the corresponding mode, which is of tearing type, appears to be invariably direct. When tearing cannot occur, the marginal state is of g–mode type, but its R_m is positive and increases with k for fixed Λ, but to zero for fixed $\mathbf{k}$ and $\Lambda \to \infty$. The marginal mode is direct if p_κ is small, but may be overstable otherwise.

The main example studied here is a sheet pinch in which $\mathbf{B}$ is of constant strength but turns uniformly in direction with height; it is force-free. The numerical integrations were checked by asymptotic methods when practicable. The corresponding problem for the non-rotating layer is considered briefly in an appendix.

KEY WORDS: resistive instability, tearing mode, rotating magnetohydrodynamics.

1. INTRODUCTION

This is the third paper of a series devoted to resistive instabilities of sheared magnetic fields in rapidly rotating fluid systems of high electrical conductivity. As such, the series represents a generalization of the better-known magnetohydrodynamic ("MHD") studies of non-rotating systems (e.g. Furth *et al*, 1963), studies that have aimed at a better understanding of the nature of instabilities to which a magnetically confined laboratory plasma may be prone. Because they do not include Coriolis forces, these "classical" investigations are usually irrelevant to systems of cosmic scale, although there are some significant similarities. In this series, we reopen the study of the instability mechanisms, with the crucial, "non-classical" difference that the Coriolis forces provide the dominant part of the inertial forces in the equation of fluid motion.

The simplest system to exhibit resistive instabilities is the sheared pinch in which the prevailing field is horizontal and turns continuously in direction with height, z, i.e.

$$\mathbf{B}_0 = B_{0x}(z)\hat{\mathbf{x}} + B_{0y}(z)\hat{\mathbf{y}}\,, \tag{1.1}$$

where (x, y, z) are Cartesian coordinates and $\hat{\mathbf{x}}$ and $\hat{\mathbf{y}}$ are the unit vectors parallel to Ox and Oy. The fluid is in solid body rotation about the vertical with angular velocity $\mathbf{\Omega} = \Omega\hat{\mathbf{z}}$, and this defines the reference frame used in the development of the theory. In this series of papers, we concentrate on a particularly simple example of (1.1), namely the force-free field,

$$\mathbf{B}_0 = B_0[\hat{\mathbf{x}}\,\cos(qz/d) + \hat{\mathbf{y}}\,\sin(qz/d)]\,, \tag{1.2}$$

(where q and B_0 are constants) in a layer confined by two impermeable walls, $z = 0$ and $z = d$. For convenience, these walls are supposed to be perfect electrical conductors.

The simplest type of instability to which (1.1) is prone is the so-called "tearing mode". This draws its energy from the magnetic field by reconnecting the field lines of (1.1). Since reconnection (or "tearing") can take place only in a fluid of nonzero resistivity $\eta = 1/\mu_0\sigma$ (where μ_0 is the permeability of free space and σ is the electrical conductivity, both in SI units) tearing does not occur unless the Elsasser number

$$\Lambda = \frac{\sigma B_0^2}{2\Omega\rho_0} = \frac{V_A^2}{2\Omega\eta}\,, \tag{1.3}$$

is finite; here $V_A = B_0/\sqrt{(\mu_0\rho_0)}$ is the Alfvén velocity, and ρ_0 is the fluid density, assumed constant, as are σ and η. The Elsasser number is the ratio, τ_η/τ_s, of the diffusive timescale $\tau_\eta = d^2/\eta$ and the dynamic timescale, which (in the case of the rapidly rotating systems studied here, in which $\Omega \gg V_A/d$) is the so-called "slow MHD timescale", $\tau_s = 2\Omega d^2/V_A^2$.

The nature of the instability is most readily comprehended in the limit $\Lambda \to \infty$. Tearing occurs only within "critical layers", of thickness $\delta = \mathrm{O}(\Lambda^{-1/4}d)$, surrounding "critical levels" defined by the zeros of

$$F = \mathbf{k}\cdot\mathbf{B}_0, \tag{1.4}$$

where $\mathbf{k}$ is the horizontal wavevector of the perturbation. In a tearing perturbation, the field lines in the neighborhood of critical levels are essentially "interchanged", with little bending.

Kuang and Roberts (1990) — hereafter referred to as "Part 1"[3]— showed that tearing instability cannot occur unless the rate at which $\mathbf{B}_0$ turns with height is sufficiently great; for field (1.2) it is necessary (but not sufficient) for tearing that $q > \pi$. In the discussion of this Section, we focus attention on the case $\pi < q < 2\pi$ in which there is at least one, but at most two, critical levels; usually we suppose that there is just one, situated at $z = z_c$.

It was shown in Part 1 that tearing occurs for disturbances of all sufficiently long wavelength ($k < q$) provided that the magnetic diffusivity is sufficiently weak [$\Lambda > \Lambda_c(\mathrm{k})$]. In addition to determining numerically the linear stability of modes at finite values of Λ, an asymptotic analysis of the limit $\Lambda \to \infty$ was presented. It was shown that the growth rate, s, of these modes is $\mathrm{O}(\tau_s^{-1/4}\tau_\eta^{-3/4})$, which is slow on the ideal timescale τ_s, so allowing reconnection adequate time to occur, but rapid on the diffusion timescale τ_η, so that the ohmic evolution of the basic state (1.1) can be ignored.

The eigenfunctions associated with tearing instabilities are almost symmetric about the critical level in the sense that

$$b_z(z - z_c) \approx b_z(z_c - z), \tag{1.5}$$

for small $|z - z_c|$, where $\mathbf{b} = \mathbf{B} - \mathbf{B}_0$ is the perturbed magnetic field. When we meet such a symmetry in this paper, we shall describe the instability as being "of tearing type", in contrast to the antisymmetry

$$b_z(z - z_c) - b_z(z_c) \approx b_z(z_c) - b_z(z_c - z), \tag{1.6}$$

characteristic of modes "of g-mode type". Here g stands for "gravitational", and refers to the instabilities that can arise when the layer is stratified and top-heavy; later g will also be used to denote the acceleration due to gravity. Following the precedent established by Furth *et al* (1963), we shall also reserve the term g-mode for situations in which there is no diffusion of density differences. In our model, in which stratification is provided by thermal expansion, this is tantamount to setting the thermal diffusivity, κ, to zero. It is the main object of this paper to study the effect of density diffusion on gravitational instabilities in the presence of a sheared magnetic field and, to distinguish these from the g-modes that arise when $\kappa = 0$, we shall call the instabilities that are present when $\kappa \neq 0$ "convective modes".

Kuang and Roberts (1991) — hereafter referred to as "Part 2" — investigated g-mode instability by both numerical and analytic methods. Using a Rayleigh number

$$R = \frac{g\beta d^2}{\rho_0 V_A^2} \tag{1.7}$$

[3]The following corrections should be made in Part 1. In (3.10) one of the two successive factors $F^{-1}D$ should be removed; in (A18), $\Gamma(\frac{1}{8})$ should be replaced by $\Gamma(\frac{1}{4})$; the right-hand sides of (A12), (A13), (A20) and (A21) should be multiplied by the factor $\frac{1}{2}[(2 - \sqrt{2})]^{1/2}$; and, the phase factors in (A12), (A13), (A20) and (A21) should be decreased by $\pi/8$, e.g. $-3\pi/16$ in (A12) should be replaced by $-5\pi/16$.

as the dimensionless measure of the upward density gradient, β, they reached the following conclusions:

1. If $R > 0$, a perturbation of any $\mathbf{k}$ is unstable, provided Λ is sufficiently great. These modes have the g-mode symmetry (1.6); in fact v_z has, for any fixed (x, y), the same sign for all z, although that sign depends on the (x, y) chosen; in other words, the convective streams pass from one boundary to the other and back;
2. If $k > q$, so that tearing cannot occur, and if R exceeds a certain k-independent critical value, R_c, the instability is ideal, i.e. it is still present in the limit $\Lambda \to \infty$. If, however, $0 < R < R_c$, the modes are resistive, i.e. the growth rate, s, of such a mode tends to zero as $\Lambda \to \infty$. In both cases, the mode of instability is direct ($\Im(s) \equiv 0$);
3. Although bouyancy is the principal energy source of instability for $k > q$, the magnetic field plays a significant role, for in its absence instabilities can exist only for sufficiently large positive R; see §95 of Chandrasekhar (1963);
4. If $k < q$ and $\Lambda > \Lambda_c$, the tearing instability would occur in the absence of buoyancy ($R = 0$), and a *bottom*-heavy density stratification is required to stabilize the layer, i.e. the mode amplifies whenever $R > R_c(\mathbf{k})$, where $R_c(\mathbf{k})$ is negative. The mode is, however, overstable ($\Im(s) \neq 0$) for $R_c(\mathbf{k}) < R < R_c'(\mathbf{k})$, for some $R_c'(\mathbf{k}) < 0$;
5. The most rapidly growing resistive modes for any $R > 0$ are modes of very small wavelength, the so-called "fast g-modes"; their growth rates are of order τ_s^{-1}, which is independent of τ_η;
6. Although the growth rate of the tearing mode increases rapidly with the number of critical levels within the layer, the growth rates of the g-modes are independent of that number.

The g-mode instability resembles Rayleigh-Taylor instability, to which it reduces in the nonmagnetic case $\mathbf{B}_0 = 0$; see Chapter X of Chandrasekhar (1963). Conclusions similar to 1 and 5 hold and the formulations share the same basic shortcomings: not only are results 1 and 5 physically untenable, but also they betray an ill-posedness in the mathematical basis. Such absurdities are easily removed by restoring density diffusion. The convective instabilities that arise when $\kappa \neq 0$ resemble those arising in the Bénard layer; see Chapter III of Chandrasekhar (1963). In addition to invalidating results 1 and 5, the presence of density diffusion profoundly affects the remaining conclusions. Introducing the (unnamed) Prandtl number, p_κ and an alternative Rayleigh number, $\widehat{R}$, defined by

$$p_\kappa = \frac{\kappa}{\eta}, \qquad \widehat{R} = \frac{\Lambda R}{p_\kappa} = \frac{g\beta d^2}{2\Omega\rho_0\kappa}, \tag{1.8, 1.9}$$

we contend below that

I. If $k > q$, so that tearing instabilities cannot occur, direct modes of instability arise, but only when $\widehat{R}$ exceeds a positive critical value, $\widehat{R}_c$. If however p_κ is sufficiently large, overstable modes may be preferred to direct modes, i.e. have a smaller value of $\widehat{R}_c$ (see §4);

II. If $k < q$ and $\Lambda > \Lambda_c$, a tearing instability would exist for $\widehat{R} = 0$ and again a bottom-heavy density stratification is required to stabilize the layer. In contrast to

the case of the g-mode, however, the numerical evidence suggests that the instability is invariably direct. For large enough Λ, the critical $\widehat{R}_c$ is more negative when there is one critical level than when there are two; this is a consequence of the greater vertical scale and lesser diffusion associated with the convection pattern of the former (see §5);

III. Modes of all sufficiently short or long wavelength are, for any given Λ, harder to excite to instability than modes of intermediate wavelength, i.e. they are not the "preferred";

IV. When $k > q$ or $\Lambda < \Lambda_c$, direct instabilities are of g-mode type. When Λ is large enough, the marginal value $\widehat{R}_m$ is again (for the reason adumbrated in II above) *larger* when there are two critical layers than when there is only one. In either case $\widehat{R}_m \propto \Lambda^{3/4}$ as $\Lambda \to \infty$.

The plan of the present paper is as follows. After setting down the basic theory in §2, we examine in §3 the direct modes of instability, using both numerical integration and asymptotic analysis. There follows a short §4 in which the overstable modes mentioned in I above are reported; the concluding §5 follows. Details of the structure of the critical layer are presented in Appendix A, and similar ideas are developed in Appendix B for the corresponding classical problem.

2. Basic equations and boundary conditions

As in Parts 1 and 2, we suppose that the rotation of the system is large, i.e. $\Omega \gg V_A/d$. We therefore adopt the magnetostrophic approximation, in which the equation of motion reduces to

$$2\rho_0 \mathbf{\Omega}\times\mathbf{V} = -\nabla P + \mathbf{J}\times\mathbf{B} + \rho_0 C\mathbf{g}\,, \tag{2.1}$$

where $\mathbf{V}$ is the fluid velocity, P is the reduced pressure (pressure divided by ρ_0 and including centrifugal forces), $\mathbf{J}$ $(= \mu^{-1}\nabla\times\mathbf{B})$ is the electric current density, and $C = \Delta\rho/\rho_0$ measures the density excess, $\Delta\rho$, of the stratification. The remaining equations are

$$\partial_t \mathbf{B} = \nabla\times(\mathbf{V}\times\mathbf{B}) + \eta\nabla^2\mathbf{B}\,, \tag{2.2}$$

$$(\partial_t + \mathbf{V}\cdot\nabla)C = \kappa\nabla^2 C\,, \tag{2.3}$$

$$\nabla\cdot\mathbf{V} = 0\,, \qquad \nabla\cdot\mathbf{B} = 0\,, \tag{2.4, 2.5}$$

where κ and η are the diffusivities of density differences and of magnetic field; ∂_t stands for the Eulerian time derivative. The Boussinesq approximation has been adopted.

The basic state whose stability is studied is one of rest in the prevailing field (1.1),

$$\mathbf{V}_0 = 0, \qquad \mathbf{B}_0 = B_{0x}\hat{\mathbf{x}} + B_{0y}\hat{\mathbf{y}}, \qquad C_0 = -\beta z/\rho_0, \qquad \ldots, \tag{2.6}$$

and its linear stability is decided from the equations obtained by writing

$$\mathbf{V} = \mathbf{V}_0 + \mathbf{v}, \qquad \mathbf{B} = \mathbf{B}_0 + \mathbf{b}, \qquad C = C_0 + c, \qquad \ldots, \tag{2.7}$$

substituting into (2.1) – (2.5), and discarding all squares and products of the perturbed variables, $\mathbf{v}$, $\mathbf{b}$, c, ... The resulting linear system is solved subject to appropriate boundary conditions at $z = 0$ and $z = d$ (see below).

It transpires that the question of linear stability can be decided through a study of the normal modes in which $\mathbf{b}$ has the form

$$\mathbf{b} \;=\; \hat{\mathbf{b}}(z)\exp[i(k_x x \;+\; k_y y) \;+\; st]\,, \tag{2.8}$$

and similarly for $\mathbf{v}$, c, ... If $\Re s \;>\; 0$ for any such mode, the system is unstable; if $\Re s \;\leq 0$ for all modes, it is linearly stable. (The carat $\hat{}$ on $\hat{\mathbf{b}}$ and other perturbed quantities will henceforward be omitted.)

In (2.8) and what follows, we transform to dimensionless variables, as defined in Parts 1 and 2. We then have

$$v_z \;=\; \frac{i}{F}\left\{\frac{1}{\Lambda}(D^2 \;-\; k^2) \;-\; s\right\} b_z\,, \tag{2.9}$$

$$j_z \;=\; \frac{\bar{F}}{F}b_z \;-\; \frac{1}{F}D\left[\frac{1}{F}\left\{\frac{1}{\Lambda}(D^2 \;-\; k^2) \;-\; s\right\}\right] b_z\,, \tag{2.10}$$

$$\begin{aligned}\omega_z \;=\; & \frac{i}{\Lambda F}\left\{2D\left(\frac{\bar{F}}{F}\right) Db_z \;+\; D^2\left(\frac{\bar{F}}{F}\right) b_z\right\} \\ & -\frac{i}{F}\left\{\frac{1}{\Lambda}(D^2 \;-\; k^2) \;-\; s\right\}\frac{1}{F}D\left[\frac{1}{F}\left\{\frac{1}{\Lambda}(D^2 \;-\; k^2) \;-\; s\right\} b_z\right]\,,\end{aligned} \tag{2.11}$$

$$D\omega_z \;-\; i[F(D^2 \;-\; k^2) \;-\; D^2 F]b_z \;+\; Rk^2 c \;=\; 0\,, \tag{2.12}$$

$$\left[\frac{p_\kappa}{\Lambda}(D^2 \;-\; k^2) \;-\; s\right] c \;=\; -v_z, \tag{2.13}$$

where $\boldsymbol{\omega} \;=\; \boldsymbol{\nabla}\mathbf{\times}\mathbf{v}$ is the vorticity, $D \;=\; d/dz$, $k \;=\; \sqrt{(k_x^2 \;+\; k_y^2)}$, and[4]

$$F = k_x B_{0x} + k_y B_{0y}, \qquad \bar{F} = k_x J_{0x} + k_y J_{0y} = D(k_y B_{0x} - k_x B_{0y})\,. \tag{2.14}$$

The system (2.9) – (2.13) differs from that solved in Part 2 only by the presence of the term proportional to p_κ/Λ in (2.13), but that difference is crucial. It accounts for the essentially dissimilar character of the convective modes from the g-modes, both physically and mathematically. In Parts 1 and 2, the governing systems were of sixth order, but here it is of eighth order. To close the problem we apply:

$$v_z = b_z = Dj_z = \;c \;=\; 0\,, \qquad \text{at} \qquad z = 0, 1\,, \tag{2.15}$$

corresponding to impermeable walls that are perfect electrical conductors and at which the fluid density is the same irrespective of whether convection occurs or not. [For example, when $\Delta\rho$ is produced by thermal expansion, the last of (2.15) states that the walls are maintained at constant temperature, c.]

Equations (2.9) – (2.15) define an eigenvalue system for the growth rate, s. For given Λ, p_κ and $\mathbf{k}$, marginal states are given by those values (R_m) of R for which $\Re s \;=\; 0$. Such bifurcations may be direct ($\Im s \;=\; 0$) or oscillatory ($\Im s \;\neq\; 0$). The critical mode for given

[4] In Part 1, $\bar{F}$ was defined with the opposite sign.

Λ and p_κ is defined by that $\mathbf{k}$ ($= \mathbf{k}_c$, say) for which R_m is smallest (and equal to R_c, say). One objective of this paper to determine R_m and $\mathbf{k}$, to explore their dependence on Λ and p_κ, deciding in each case whether the bifurcation is direct or oscillatory. Another objective is to develop an asymptotic theory of convective instabilities in the limit of large Λ.

By elimination between (2.9) and (2.13), we find that

$$\left[\frac{p_\kappa}{\Lambda}(D^2 - k^2) - s\right]\left\langle D\left[\left[\frac{1}{F}\left\{\frac{1}{\Lambda}(D^2-k^2)-s\right\}\frac{1}{F}D\left[\frac{1}{F}\left\{\frac{1}{\Lambda}(D^2-k^2)-s\right\}b_z\right]\right]\right.\right.$$
$$\left.\left. -\frac{1}{\Lambda}D\left[\frac{1}{F}\left\{2D\left(\frac{\bar{F}}{F}\right)Db_z + D^2\left(\frac{\bar{F}}{F}\right)b_z\right\}\right] + F(D^2-k^2)b_z - (D^2F)b_z\right\rangle$$
$$+ \frac{Rk^2}{F}\left\{\frac{1}{\Lambda}(D^2-k^2) - s\right\}b_z = 0, \qquad (2.16)$$

together with the four very complicated boundary conditions on b_z at each wall implied by (2.15). Equation (2.16) is useful in studying limiting cases, such as $\Lambda \to \infty$ and/or $p_\kappa \to \infty$.

If we write

$$k_x = -k\sin\theta, \qquad k_y = k\cos\theta, \qquad (2.17)$$

we have, for the field (1.2),

$$F = -\bar{F}/q = k\sin q(z - z_c), \qquad \text{where} \qquad z_c = \theta/q, \qquad (2.18)$$

and the first combination of terms on the right-hand side of (2.11) is absent, as are the $\bar{F}$ terms in (2.16). The $\bar{F}$ term remaining in (2.10) nevertheless destroys, through the third term of (2.15), the symmetry or antisymmetry of the eigenfunctions even when F is symmetric about the mid-plane [$F(z) \equiv F(1-z)$]. This is particularly evident when j_z is graphed; see the discussion in Part 1.

In what follows, as in Part 1, much hinges on the behavior of the solutions in the "critical layers", regions that are narrow when Λ is large, and which surround the "critical levels" at which F vanishes. In Part 2 we distinguished four possibilities:

A. there are no critical levels; F has no zero in $0 < z < 1$;
B. there is one critical level in $0 < z < 1$, namely $z = z_c$;
C. there are two critical levels in $0 < z < 1$, namely $z = z_1$ and $z = z_1 + \pi/q = z_2$ (say), at both of which $\mathbf{k}$ is orthogonal to $\mathbf{B}_0$;
D. there are three or more critical levels in $0 < z < 1$.

Tearing instabilities cannot occur in case A, and also cannot arise in the other cases unless k is small enough. Attention was therefore focussed in Part 1 on cases B and C; case D was excluded because it added complications without enlightenment. In Part 2 instability always arose for positive R (and for negative R also in cases B and C, when k and Λ are in the tearing range), and case A was therefore investigated. Convective instabilities ($p_\kappa \neq 0$) of type A arise only if R is sufficiently positive; in fact, $R_m > 0$ and $R_m \to$ constant as $\Lambda \to \infty$. In this respect the instabilities resemble those that arise when $\mathbf{B}$ is uniform (and $\mathbf{k}\cdot\mathbf{B}_0 \neq 0$). In cases B and C this instability is assisted by the

presence of the critical layers, i.e. their R_m lies below that obtained in case A for the same $\mathbf{k}$. Case A is therefore irrelevant, and we shall not consider it in this paper. Of course, tearing instabilities are governed by the present theory when $R = 0$, and instabilities very similar to the tearing modes arise when R is sufficiently small. We shall, however, not go over the same ground as that covered in Part 1. Once more, we shall not examine case D.

3. Direct Modes

3.1 Numerical Results

In this Section we suppose that the principle of the exchange of stability holds, i.e. that the marginal modes are direct: $s = 0$. Equations (2.9) – (2.15) then define an eigenvalue problem for the marginal Reynolds number, $R_m(\mathbf{k})$. The minimum of that function over $\mathbf{k}$, which is achieved for $\mathbf{k} = \mathbf{k}_c$ and $R(\mathbf{k}_c) = R_c$ (say), defines the critical mode. This is the mode for which steady convection can first occur as R is gradually increased from a large negative value. In many convection problems it is the first mode for which convection can occur as R is increased from zero, but we may recall (see Part 1) that the layer is unstable to tearing modes ($R = 0$) for all sufficiently small k and all sufficiently large Λ. In such situations, a top-heavy density distribution makes the mode even more unstable; the layer must be *bottom*-heavy when the convection is marginal, i.e. $R_m < 0$.

Figure 1 shows $-R_c/p_\kappa$ and k_c for $q = \frac{3}{2}\pi$ as a function of Λ for $\Lambda \leq 3000$. In this range, the most unstable mode has, as in the case of the tearing mode considered in Part 1, two critical levels, and the location of one of these is also shown in Figure 1. Unlike the case of the tearing mode, in which one critical level or the other appeared to move systematically towards a boundary layer as Λ increased, the critical level for the convective mode moves away, then briefly towards, then again away from the boundary before finally moving systematically towards it. It seems probable that ultimately, as in the case $R = 0$, this critical level eventually moves into the boundary layer. We have not established this unequivocally, and it does not seem to us to be of great interest since, as Λ is increased sufficiently, the preferred mode switches to one having a single critical layer; see below.

3.2 The limit $\Lambda \to \infty$; general case

In this subsection we examine the structure of solutions in the limit $\Lambda \to \infty$ and determine the order of magnitude of the marginal R. Surrounding each critical level, there exists a critical layer, of thickness δ (say); abutting $z = 0$ and $z = 1$ there are boundary layers of thickness $\Lambda^{-1/2}$. Between these two types of "inner region" lie the "outer regions" in which to leading order we may set Λ^{-1} to zero in the governing equations. We then find from (2.16) that b_z obeys the fourth order equation

$$(D^2 - k^2)\left[F(D^2 - k^2)b_z - (D^2F)b_z\right] + \frac{R_m k^2}{p_\kappa F}(D^2 - k^2)b_z = 0. \qquad (3.1)$$

Provided we solve (3.1) subject to

$$b_z = D^2 b_z = 0, \qquad \text{at} \qquad z = 0, 1, \qquad (3.2)$$

we may construct boundary layers at $z = 0$ and 1 that match to these outer solutions

and also obey conditions (2.15). It is easily seen that, as the critical layer is approached,

$$b_z \sim \begin{cases} A^+ + B^+(z-z_c) + E^+(z-z_c)^{\alpha_1} + G^+(z-z_c)^{\alpha_2}, & z \to z_c+, \\ A^- + B^-(z-z_c) + E^-(z_c-z)^{\alpha_1} + G^-(z_c-z)^{\alpha_2}, & z \to z_c-, \end{cases} \tag{3.3}$$

where $A^\pm$, $B^\pm$, $E^\pm$ and $G^\pm$ are constants, as are

$$\alpha_1 = \tfrac{3}{2} + \left(\tfrac{1}{4} - \widehat{r}_m\right)^{1/2}, \qquad \alpha_2 = \tfrac{3}{2} - \left(\tfrac{1}{4} - \widehat{r}_m\right)^{1/2}, \tag{3.4}$$

and

$$\widehat{r} = \frac{Rk^2}{p_\kappa F_c'^2}, \tag{3.5}$$

where $F_c' = F'(z_c)$; we suppose that $\widehat{r} < \frac{1}{4}$.

To connect the outer solutions across the critical layer, it is necessary to solve (2.16) in the inner, or "critical", layer surrounding $z = z_c$. The thickness of this critical layer is $O(\delta)$ where, as in Parts 1 and 2,

$$\delta = \frac{1}{\Lambda^{1/4}|F_c'|^{1/2}}. \tag{3.6}$$

We therefore introduce the stretched coordinate ζ by writing

$$\zeta = \frac{z-z_c}{\delta}, \qquad \alpha = -\frac{\overline{F}_c}{F_c'}, \tag{3.7}$$

and find from (2.16) that b_z is governed to leading order in the critical layer by

$$D^2\left\{\left[D\left(\frac{1}{\zeta}D^2\right)\left(\frac{1}{\zeta}D\right) + \zeta^2\right]\left(\frac{1}{\zeta}D^2\right)b_z + 2\alpha D\left[\frac{1}{\zeta^2}D\left(\frac{b_z}{\zeta}\right)\right]\right\} + \widehat{r}\left(\frac{1}{\zeta}D^2\right)b_z = 0, \tag{3.8}$$

where now $D = d/d\zeta$. In what follows we shall, for simplicity, suppose that $\alpha = 0$, as is indeed true for model (1.2).

It is easily seen from (3.8) that, as $\zeta \to +\infty$,

$$\begin{aligned} b_z \sim\ & C_1^+ + C_2^+\zeta + C_3^+\zeta^{\alpha_1} + C_4^+\zeta^{\alpha_2} \\ & + C_5^+\zeta^{-3/2}\mathrm{e}^{-\zeta^2/2\sqrt{2}}\cos(\zeta^2/2\sqrt{2}) + C_6^+\zeta^{-3/2}\mathrm{e}^{-\zeta^2/2\sqrt{2}}\sin(\zeta^2/2\sqrt{2}) \\ & + C_7^+\zeta^{-3/2}\mathrm{e}^{\zeta^2/2\sqrt{2}}\cos(\zeta^2/2\sqrt{2}) + C_8^+\zeta^{-3/2}\mathrm{e}^{\zeta^2/2\sqrt{2}}\sin(\zeta^2/2\sqrt{2}), \end{aligned} \tag{3.9}$$

for some constants C_i^+, $i = 1-8$. Similarly, for $\zeta \to -\infty$,

$$\begin{aligned} b_z \sim\ & C_1^- + C_2^-\zeta + C_3^-(-\zeta)^{\alpha_1} + C_4^-(-\zeta)^{\alpha_2} \\ & + C_5^-(-\zeta)^{-3/2}\mathrm{e}^{-\zeta^2/2\sqrt{2}}\cos(\zeta^2/2\sqrt{2}) + C_6^-(-\zeta)^{-3/2}\mathrm{e}^{-\zeta^2/2\sqrt{2}}\sin(\zeta^2/2\sqrt{2}) \\ & + C_7^-(-\zeta)^{-3/2}\mathrm{e}^{\zeta^2/2\sqrt{2}}\cos(\zeta^2/2\sqrt{2}) + C_8^-(-\zeta)^{-3/2}\mathrm{e}^{\zeta^2/2\sqrt{2}}\sin(\zeta^2/2\sqrt{2}). \end{aligned} \tag{3.10}$$

We are required to match (3.9) and (3.10) to (3.3), and it is at once clear that

$$\begin{aligned} C_7^{\pm} &= C_8^{\pm} = 0, \\ C_1^{\pm} &= A^{\pm}, \quad C_2^{\pm} = B^{\pm}\delta, \\ C_3^{\pm} &= E^{\pm}\delta^{\alpha_1}, \quad C_4^{\pm} = G^{\pm}\delta^{\alpha_2}. \end{aligned} \tag{3.11}$$

In view of (3.11), it is clearly convenient to find four fundamental solutions of (3.8) that lack exponentially growing terms as $|\zeta| \to \infty$, and are therefore algebraic, apart from exponentially small terms. In fact, two such solutions are immediate and exact:

$$b_1(\zeta) = 1, \qquad b_2(\zeta) = \zeta. \tag{3.12}$$

In Appendix A, two further solutions of (3.8) are derived, one odd in ζ and one even. For these

$$b_e(\zeta) \sim K_e|\zeta|^{\alpha_1} + L_e|\zeta|^{\alpha_2}, \qquad |\zeta| \to \infty, \tag{3.13}$$

$$b_o(\zeta) \sim [K_o|\zeta|^{\alpha_1} + L_o|\zeta|^{\alpha_2}]\,\mathrm{sgn}(\zeta), \qquad |\zeta| \to \infty. \tag{3.14}$$

(We have omitted exponentially small terms.) The ratios L_e/K_e and L_o/K_o are known functions of $\widehat{r}_m$ determined by the analysis of the critical layer (Appendix A). We now seek to match (3.3) to

$$b_z = C_1 b_1 + C_2 b_2 + F_e b_e + F_o b_o, \tag{3.15}$$

and it is apparent from (3.13) and (3.14) that

$$C_1 = A^{\pm}, \quad C_2 = B^{\pm}\delta, \tag{3.16}$$

$$F_e K_e \pm F_o K_o = E^{\pm}\delta^{\alpha_1}, \quad F_e L_e \pm F_o L_o = G^{\pm}\delta^{\alpha_2}. \tag{3.17}$$

These four conditions on $A^{\pm}$, $B^{\pm}$, $E^{\pm}$ and $G^{\pm}$ link the solution across the critical level and close the eigenvalue problem.

3.3 The limit $\Lambda \to \infty$; g-type modes

It was shown in Part 2 that the g–modes of short wavelength are the most unstable. When $p_\kappa \neq 0$, the situation is quite different – the short wavelength modes of g–type are more stable than those of tearing type that exist only at longer wavelengths; in fact, R_m is positive and increases with k for fixed $\mathbf{k}/k$ and Λ. Nevertheless, the magnetic field helps to promote the instability, in the sense that, when a critical level exists, $R_m \to 0$ as $\Lambda \to \infty$ for fixed $\mathbf{k}$.

Because of the totally different nature of the modes of g–type when $p_\kappa \neq 0$, we analyze these further below. Anticipating the final result, we suppose that $\widehat{r}_m = o(1)$ as $\Lambda \to \infty$; we shall verify the self-consistency of this assumption *a posteriori*. By (3.4) we have

$$\alpha_1 \approx 2 - \widehat{r}_m, \qquad \alpha_2 \approx 1 + \widehat{r}_m. \tag{3.18}$$

Thus, in the limit $\widehat{r}_m \to 0$, the solution involving α_2 ceases to be independent of the solution linear in $z - z_c$ near $z = z_c$, and from their difference logarithmic terms arise in b_z both in the inner and outer expansions, as we shall see. Also, as is shown in Appendix A,

$$\frac{L_o}{K_o} \sim \frac{\lambda_o}{\widehat{r}_m^2} \doteq -\frac{0.7137821}{\widehat{r}_m^2}, \qquad \frac{L_e}{K_e} \sim \lambda_e \doteq -3.006535, \qquad \widehat{r} \to 0. \tag{3.19}$$

We may solve (3.17) to obtain

$$G^+ = -G^- = \tfrac{1}{2}\lambda_o\delta(E^+ - E^-) = \lambda_o F_o K_o/\delta. \tag{3.20}$$

This demonstrates that b_o completely dominates b_e in (3.15) and that

$$b_z \sim C_1 + \frac{C_2}{\delta}(z - z_c) + F_o K_o \left[(z - z_c)^2 + \frac{\lambda_o\delta}{\widehat{r}_m^2}|z - z_c|^{1+\widehat{r}_m}\right] \mathrm{sgn}(z - z_c), \tag{3.21}$$

which, in terms of new constants, can be written as

$$b_z \sim C_1 + C_2(z - z_c) + C_3\left[\frac{\lambda_o\delta}{\widehat{r}_m}(z - z_c)\ln|z - z_c| + (z - z_c)^2\mathrm{sgn}(z - z_c)\right]. \tag{3.22}$$

In particular, this implies that

$$b_z(z_c+) = b_z(z_c-) = b_{zc}, \quad \text{say,} \tag{3.23}$$

$$\frac{d^2 b_z}{dz^2} = C_3\left[\frac{\lambda_o\delta}{\widehat{r}_m(z - z_c)} \pm 2\right], \qquad \text{for} \qquad z \to z_c\pm, \tag{3.24}$$

from which it follows that

$$\lim_{z \to z_c\pm}(z - z_c)\frac{d^2 b_z}{dz^2} = \frac{\lambda_o\delta}{4\widehat{r}_m}\left[\frac{d^2 b_z}{dz^2}\right]_{z_c-}^{z_c+}. \tag{3.25}$$

The fact that $(z - z_c)d^2 b_z/dz^2$ tends to a common limit as $z \to z_c$ from either side means that the right-hand side of (3.25) is properly defined.

It is easy to apply (3.25) in cases where, as for model (1.2), D^2F vanishes with F at $z = z_c$. Suppose that there is only one critical level within the layer. Since, by assumption, $|\widehat{r}_m| \ll 1$, we may find the outer solutions to leading order by neglecting the final term in (3.1) and obtain, using also (3.2),

$$F(D^2 - k^2)b_z - (D^2F)b_z = \begin{cases} C_4^+ \sinh k(1 - z), & \text{for} \quad z_c < z \le 1, \\ C_4^- \sinh kz, & \text{for} \quad 0 \le z < z_c. \end{cases} \tag{3.26}$$

Applying (3.25), we now obtain, with the help also of (3.6) and (3.19),

$$\widehat{r}_m \sim \frac{0.1784455}{|F_c'|^{1/2}} \frac{k \sinh k}{\sinh kz_c \sinh k(1 - z_c)} \Lambda^{-1/4}, \qquad \Lambda \to \infty. \tag{3.27}$$

According to (3.28), the minimum $\widehat{r}_m$ as a function of z_c occurs when $z_c = \frac{1}{2}$, i.e. when the critical level is central. Then

$$\widehat{r}_m \doteq \frac{0.3568910}{|F_c'|^{1/2}} \left(k \coth \frac{1}{2}k\right) \Lambda^{-1/4}. \tag{3.28}$$

Recalling that F_c' is proportional to k, we see that, as a function of k, $\widehat{r}_m$ has a single minimum for $k \doteq 2.177319$. This leads to

$$\widehat{r}_c \sim \frac{0.6612592}{|F_c'/k|^{1/2}} \Lambda^{-1/4}, \qquad \Lambda \to \infty. \tag{3.29}$$

It may be noted that $\widehat{r}_m = O(k^{1/2}\Lambda^{-1/4}) \to \infty$ for $k \to \infty$, and $\widehat{r}_m = O(k^{-1/2}\Lambda^{-1/4}) \to \infty$ for $k \to 0$.

It is straightforward in principle to extend the argument just given to the case of two critical levels, $z = z_1$ and $z = z_2 = z_1 + \pi/q$, and it is found that, in place of (3.27), we have

$$\widehat{r}_m \sim \frac{0.1784455}{|F_c'|^{1/2}} kX \Lambda^{-1/4}, \qquad \Lambda \to \infty, \tag{3.30}$$

where X is the smaller of the two positive roots of

$$X^2 - \left(\frac{\sinh kz_2}{\sinh kz_1} + \frac{\sinh k(1-z_1)}{\sinh k(1-z_2)}\right) X + \frac{\sinh k \sinh k\pi/q}{\sinh kz_1 \sinh k(1-z_2)} = 0. \tag{3.31}$$

An investigation of this case shows that, in contrast to the behavior of both the tearing-type modes and the g–modes (in which the growth rate is independent of the number of critical levels, provided there is at least one), it is *harder* to excite convective modes that have two critical levels than to excite a mode having only one. This is brought out in Figure 2 which shows R_m/p_κ as a function of k_y/k for fixed $k = 4\sqrt{2}$ and $k_x > 0$; here $q = \frac{3}{2}\pi$ and $\Lambda = 10^6$. The minimum value of R_m occurs for $k_x = k_y = 4$ (one centrally placed critical mode), and the maximum for $k_x = -k_y = 4$ (the case of two symmetrically–placed critical modes, at $z_1 = \frac{1}{6}$ and $z_2 = \frac{5}{6}$). The ratio of maximum to minimum is approximately 1.144; the asymptotic results (3.28) and (3.30) give 1.148.[5]

The situation is further illustrated in Figure 3, in which the cases of one and two critical levels are shown for the same value of k. The asymptote ($R_m/p_\kappa \sim 8.74418\Lambda^{-1/4}$) given by (3.28) is also drawn, but the asymptote for the corresponding case of two critical levels ($R_m/p_\kappa \sim 10.04112\Lambda^{-1/4}$) is omitted for clarity. The corresponding eigenfunctions are shown in Figure 4. These should be contrasted with those shown for the tearing-type mode in Figure 7 below.

Another case in which tearing is impossible arises when the basic field turns in direction too slowly with height z (see Part 1). Again $\widehat{r}_m \to 0$ as $\Lambda \to \infty$ and the theory developed here applies. This is illustrated in Figure 5.

[5] As in Part 1, the correction terms to (3.28) and (3.30) are positive and of order $\Lambda^{-1/4}$ times smaller than the leading terms evaluated above. As a result, the values 0.276515 and 0.317527 of $\Lambda^{1/4}\widehat{r}_m$ given by (3.28) and (3.30) for the extrema are too small (by 7–8% for $\Lambda = 10^6$).

3.4 The limit $\Lambda \to \infty$; Tearing-type modes

When tearing-type modes become possible, they are also preferred over the g–type modes, and the situation is quite different from that described in §3.3 above. Now R/p_κ tends to a finite limit as $\Lambda \to \infty$. The theory of the critical level developed in §3.2 applies as before, and the matching is again to an outer solution that obeys the fourth order equation (3.1) and (3.2). Now however $\widehat{r}_m = O(1)$, and (3.1) is no longer degenerate and easily soluble. The difficulty of obtaining the asymptotic answer is scarcely less than that of obtaining a full numerical solution at large Λ; we therefore only investigated the case numerically. In Figure 6 we show $-R_m/p_\kappa$ as a function of Λ both for the case of one centrally-placed critical level and for the case of two symmetrically placed critical levels when $q = \frac{3}{2}\pi$. It will be seen that, for sufficiently large Λ, the modes with two critical levels require a smaller negative R_m to stabilize them, i.e. the modes having one critical level are again the more unstable. The corresponding eigenfunctions are shown in Figure 7. These should be contrasted with those shown in Figure 4. The totally different structures of g-type and tearing-type modes is obvious.

3.5 The limit $\Lambda \to \infty$; Summary

The salient facts that have emerged from this analysis are

(1) When the marginal value of $\widehat{r}$ tends to zero as $\Lambda \to \infty$, that marginal value is positive, i.e. it refers to a g-type mode and not to a tearing-type mode;
(2) Consistent with this conclusion, the solution in the neighborhood of the critical level is nearly odd, i.e. $v_z(z - z_c) \doteq -v_z(z_c - z)$;
(3) Small wavelength instabilities are quenched by the presence of thermal diffusion, and are not maximally unstable, as was the case for the g-modes studied in Part 2;
(4) Since the marginal $\widehat{r}$ is negative for tearing-type modes, such marginal $\widehat{r}$ cannot tend to zero as $\Lambda \to \infty$, and (as the numerical results indicate) they in fact tend to finite (negative) values in that limit;
(5) The mode with one critical layer is always more unstable than the mode with two critical layers. This conclusion holds irrespective of whether the mode is of tearing type or $g-$type. (For small Λ, this conclusion is reversed; see §3.1.)

4. Overstable Modes

It was shown in Part 2 that, when tearing can occur, the marginal mode is overstable. It appears that this conclusion holds true *only* when $p_\kappa = 0$. In all cases we integrated for $p_\kappa \neq 0$, the marginal mode is direct in the tearing range. Curiously, however, in conditions under which tearing can *not* occur, and for which we found the g–modes of Part 2 to be invariably direct, overstable convective modes may exist when p_κ is sufficiently large, when Λ is neither too small *nor* too large, and when only one critical level exists. This stands in sharp contrast to the behavior of systems having no critical layers for which $F(z)$ is nowhere zero, and for which overstability occurs (when p_κ is large enough) for *all* sufficiently large Λ; see §5. Numerical evidence for an upper limit, $\Lambda^*(p_\kappa)$, for overstability is presented in Figures 8 and 9, in which $p_\kappa = 5$ and 10, respectively, and in both cases $k_x = k_y = 4$ and $q = \frac{3}{2}\pi$. For these examples

$$\Lambda^*(5) \approx 129.99, \qquad \Lambda^*(10) \approx 3888.3. \tag{4.1}$$

It seems very probable that $\Lambda^*(p_\kappa)$ increases indefinitely with p_κ.

Overstable modes do not exist once the Rayleigh number, R, exceeds that of a second branch of the dispersion relationship, which is shown by the dashed and dotted curve in Figures 9 and 10. The numerical evidence is strong that this branch terminates precisely on the marginal curve for steady convection. At this codimension-2 point, the frequency, $\Im(s)$, of the overstable mode is zero. Many hydrodynamical systems exhibit analogous bifurcation structures. As in our case, the preference for a steady bifurcation (a direct mode) over a Hopf bifurcation (overstability), or the reverse, is decided by an external control parameter, such as the separation ratio in thermohaline convection (Brand and Sternberg, 1983) or such as the Prandtl number p_κ in magnetoconvection (Chandrasekhar, 1961; Proctor and Weiss, 1982). In some of these cases, the instabilities have been analyzed at finite amplitude, and the behavior of solutions near the codimension-2 point has been elucidated. For example, Knobloch and Weiss (1981) showed by singular perturbation methods that, if the direct mode branch is subcritical, the overstable branch terminates on it, and that the period of the oscillatory solutions tends to infinity as it did so ($\Im(s) = 0$). In this case, the overstable mode is represented by a heteroclinic orbit that connects the two unstable steady branches, corresponding to positive and negative amplitudes. We presume that weakly nonlinear disturbances would behave analogously in our system, but we have not verified this.

The fact that $\Im(s) \to 0$ on the overstable branch as the codimension-2 point is approached is a consequence of chosing the wave vector (here $k_x = k_y = 4$) to be the same for both the direct and overstable modes. In systems usually considered, the wavevectors are chosen to minimize R_m separately for the direct and overstable modes, and the resulting $\mathbf{k}$ are different at the codimension-2 point where the two values of R_c coincide; consequently $\Im(s)$ on the overstable branch is nonzero at that point. In such cases, interesting questions arise concerning the spatial modulation of disturbances (e.g. Zimmermann *et al*, 1988). In our system, R_c lies in the tearing range where no overstability occurs, and it seems pointless to examine such questions.

5. Conclusions

As in Part 2, we have found that the presence of critical layers has a strong effect on the convective stability of the sheet pinch. We have shown that the critical layer of a tearing-type mode is not drastically modified by the presence of buoyancy, and in particular possesses the same symmetry (1.5). The inherent instability of a tearing mode can be neutralized only by a bottom heavy distribution, requiring that R_m be negative, as we have confirmed.

When $p_\kappa \neq 0$, the critical layer of g–type has been found to have quite a different structure from the one analyzed in Part 2, for which $p_\kappa = 0$, although its antisymmetry (1.6) is preserved. Two consequences of the altered structure are these: (i) the rapidly growing fast g–modes of Part 2 are completely absent, and (ii) R_m (which is now positive) increases rapidly with wavenumber k for fixed Λ. Nevertheless (iii) R_m, considered as a function of Λ for fixed k, tends to zero as $\Lambda \to \infty$. Another striking difference from Part 2 is that, when $p_\kappa = 0$, critical layers do not interact, i.e. the growth rate of the g–mode is almost the same for one critical layer as for many. When $p_\kappa \neq 0$, this is no longer

true; the critical layers "interact". These dramatic reversals of the conclusions of Part 2 has motivated us to pay particular attention in this paper to the fate of g–modes when $p_\kappa \neq 0$ and to confirm the statements just made.

Concerning the decrease of R_m with increasing Λ for fixed $\mathbf{k}$ just mentioned, we should point out that, when no critical layer is present, the system behaves in much the same way as does a layer with a constant horizontal $\mathbf{B}_0$, assuming of course that $\mathbf{k}$ is not perpendicular to it; in fact, supposing for simplicity that $\mathbf{k}$ and $\mathbf{B}_0$ are parallel, we find In the case of the direct modes that

$$\frac{R_m}{p_\kappa} = B_0^2(\pi^2 + k^2) + \frac{\pi^2}{B_0^2}\frac{(\pi^2 + k^2)^2}{k^4\Lambda^2}, \tag{5.1}$$

which obviously tends to a constant as $\Lambda \to \infty$.

The overstable modes provide another illustration of the importance of critical levels. In the case of constant $\mathbf{B}_0$ just considered, it is easily shown that

$$\frac{R_m}{p_\kappa} = \frac{2B_0^2}{p_\kappa(p_\kappa + 1)}(\pi^2 + k^2) + \frac{2\pi^2}{B_0^2}\frac{(p_\kappa + 1)}{p_\kappa}\frac{(\pi^2 + k^2)^2}{k^4\Lambda^2}, \tag{5.2}$$

$$\omega^2 = k^4 B_0^4 \frac{(p_\kappa - 1)}{(p_\kappa + 1)}\frac{(\pi^2 + k^2)}{\pi^2} - \frac{(\pi^2 + k^2)^2}{\Lambda^2}, \tag{5.3}$$

where $\omega = \Im(s)$ is the oscillation frequency. Again, R_m does not tend to zero as $\Lambda \to \infty$, but unstable modes exist whenever $p_\kappa > 1$ for *all* sufficiently large Λ; there is no upper bound $\Lambda^*(p_\kappa)$, such as we located in §4 for a system having a critical level.

Finally, a striking reversal of one of the conclusions of Part 1 deserves comment, namely the fact that (for large enough Λ) the convective mode is *more* stable when there are two critical layers than when there is only one, whereas for the tearing mode the opposite is true. Figures 10 throws some light on this phenomenon. These show the isolines of the non-dimensional density perturbation, c, for the tearing-type perturbations both (a) when there is a central critical level and (b) when there are two symmetrically-placed critical levels. Only the ξz–section is shown where ξ is the horizontal coordinate parallel to $\mathbf{k}$, and z is the vertical height. It will be seen that the variation in density is on a smaller vertical scale in (b) than in (a), corresponding to the fact that in (b) there are three circulating cells in the vertical whereas in (a) there are only two. Shorter length scales[6] are associated with higher diffusion rates of c and $\mathbf{b}$, and larger values of R_m result. Similar conclusions may be drawn from Figures 11, which show corresponding results for convective modes of g–type. Figures 10 and 11 also well exemplify, for c rather than b_z, the symmetries (1.5) and (1.6) mentioned in §1.

Acknowledgements We are grateful to the National Science Foundation for support under grant EAR-8846267.

[6] Although the central cell in (b) is larger than either cell in (a), this cell has to drive into motion the two small cells above and below it, and overcome their diffusive drag.

References

Brand, H.R. and Steinberg, "Convective instabilities in binary mixtures in a porous medium," *Physica* **118***A*, 327–328 (1983).
Chandrasekhar, S., *Hydrodynamic and Hydromagnetic Stability.* Oxford: University Press (1961).
Furth, H.P, Killeen, J. and Rosenbluth, M.N., "Finite resistive instabilities of a sheet pinch," *Phys. Fluids* **6**, 459–484 (1963).
Knobloch, E. and Proctor, M.R.E., "Nonlinear periodic convection in double–diffusive systems," *J. Fluid Mech.* **108**, 291–316 (1981).
Kuang, W. and Roberts, P.H., "Resistive instabilities in rapidly rotating fluids: linear theory of the tearing mode," *Geophys. Astrophys. Fluid Dynam.* **55**, 183–223 (1990).
Kuang, W. and Roberts, P.H., "Resistive instabilities in rapidly rotating fluids: linear theory of the g–mode," *Geophys. Astrophys. Fluid Dynam.* **60**, 295–333 (1991).
Proctor, M.R.E. and Weiss, N.O., "Magnetoconvection," *Rep. Prog. Phys.*, **45**, 1317–1379 (1982).
Zimmermann, W., Armbuster, D., Kramer, L. and Kuang, W. "The effect of spatial modulation on codimension –2 bifurcation," *Europhys. Lett.* **6**, 505–510 (1988).

Appendix A. Analysis of the Critical Layer for $\alpha = 0$

The critical layer is governed by the eighth order equation (3.8) which (for $\alpha = 0$) is

$$D^2\left[D\left(\frac{1}{\zeta^2}D\right)(\zeta^2 D)\left(\frac{1}{\zeta^2}D\right) + \zeta^2\right]\left(\frac{1}{\zeta}D^2 b\right) + \widehat{r}_m\left(\frac{1}{\zeta}D^2 b\right) = 0\,. \qquad \text{(A1)}$$

Here $D = d/d\zeta$. We at first suppose that $0 < \widehat{r}_m < \frac{1}{4}$. It is easily seen that (A1) admits solutions that are even or odd in ζ, the simplest being

$$b_1 = 1\,, \qquad b_2 = \zeta\,. \qquad \text{(A2)}$$

As explained in §3.2, we require two further solutions that contain no exponentially large terms in the limit $\zeta \to \infty$. We shall generate two such solutions, one ($\tilde{b}_o$) odd in ζ and the other ($\tilde{b}_e$) even in ζ, with the property that, apart from exponentially small terms,

$$\tilde{b}_o \sim (K_o|\zeta|^{\alpha_1} + L_o|\zeta|^{\alpha_2} + M_o|\zeta|)\ \text{sgn}\ \zeta\,, \quad \zeta \to \pm\infty\,, \qquad \text{(A3)}$$

$$\tilde{b}_e \sim K_e|\zeta|^{\alpha_1} + L_e|\zeta|^{\alpha_2} + M_e\,, \qquad \zeta \to \pm\infty\,, \qquad \text{(A4)}$$

where α_1 and α_2 are defined in (3.4). Matching to the outer solution requires knowledge of K_o/L_o and K_e/L_e. It is the principal objective of this Appendix to evaluate these constants.

It is a simple matter to find six solutions of (A1) of the form

$$b_i = \sum_{n=0}^{\infty} \frac{(-1)^n\,\tilde{\gamma}(-\alpha_1)\,\tilde{\gamma}(-\alpha_2)\,(\zeta/2^{3/2})^{m_i+8n}}{\tilde{\gamma}(-2)\,\tilde{\gamma}(2)\,\tilde{\gamma}(3)\,\tilde{\gamma}(5)\,\tilde{\gamma}(7)\,\tilde{\gamma}(8)}\,, \qquad \text{(A5)}$$

where $i = 3-8$ and

$$m_3 = 3, \quad m_4 = 5, \quad m_5 = 6, \quad m_6 = 8, \quad m_7 = 9, \quad m_8 = 10\,. \tag{A6}$$

We have used the abbreviations

$$\tilde{\gamma}(k) \;=\; \gamma(m_i \;+\; 8n \;+\; k), \qquad\qquad \gamma(k) \;=\; \Gamma\left(\tfrac{1}{8}k\right),$$

the second of which is employed frequently in this Appendix. Note that, according to (A2), (A5) and (A6),

$$\left.\begin{aligned} b_i(-\zeta) &= -b_i(\zeta), \qquad \text{for} \qquad i = 2,3,4,7, \\ b_i(-\zeta) &= \;\; b_i(\zeta), \qquad \text{for} \qquad i = 1,5,6,8. \end{aligned}\right\} \tag{A7}$$

To determine the dominant behavior of b_i as $\zeta \to +\infty$ we may proceed as in Appendix A of Part 1, replacing (A5) by a contour integral and distorting the contour to pass over saddles situated near $\frac{1}{8}\zeta^2 e^{\pm i\pi/4}$ in a complex s-plane. We obtain ($i = 3-8$)

$$b_i \sim \frac{1}{(2\pi)^{3/2}}\left(\frac{8}{\zeta^2}\right)^{3/4} \mathrm{e}^{\zeta^2/2\sqrt{2}} \cos\left[\frac{\zeta^2}{2\sqrt{2}} - \left(m_i + \frac{3}{2}\right)\frac{\pi}{8}\right], \qquad \zeta \to +\infty\,. \tag{A8}$$

This shows that we should introduce

$$b_o = b_3 - \frac{1}{\sqrt{2}}\,b_4 + \frac{1}{\sqrt{2}}\,b_7\,, \qquad b_e = \frac{1}{\sqrt{2}}\,b_5 - b_6 + \frac{1}{\sqrt{2}}\,b_8\,, \tag{A9}$$

since these contain no exponentially large terms in their asymptotic expansions. Solutions (A9) are more expeditiously written as

$$\tilde{b}_o = \Re(B_o)\,, \qquad \tilde{b}_e = \Re(B_e)\,, \tag{A10}$$

where

$$B_o = \mathrm{e}^{-\frac{9}{8}i\pi} \sum_{m=1}^{\infty} \frac{\gamma(2m+1-\alpha_1)\gamma(2m+1-\alpha_2)\left(\frac{1}{8}\zeta^2 \mathrm{e}^{3i\pi/4}\right)^{m+1/2}}{\gamma(2m-1)\gamma(2m+3)\gamma(2m+4)\gamma(2m+6)\gamma(2m+8)\gamma(2m+9)}, \tag{A11}$$

$$B_e = \sum_{m=3}^{\infty} \frac{\gamma(2m-\alpha_1)\gamma(2m-\alpha_2)\left(\frac{1}{8}\zeta^2 \mathrm{e}^{3i\pi/4}\right)^{m+1/2}}{\gamma(2m-2)\gamma(2m+2)\gamma(2m+3)\gamma(2m+5)\gamma(2m+7)\gamma(2m+8)}. \tag{A12}$$

The method we use to evaluate K_o, L_o, K_e and L_e from (A11) and (A12) parallels that employed in Appendix A of Part 1. Since $\alpha_1 > \alpha_2 > 1$ for $\widehat{r}_m \;>\; 0$, (A3) and (A4) imply that

$$K_p = \mathrm{Lt}_{\zeta\to+\infty}\zeta^{-\alpha_1}\tilde{b}_p\,, \qquad p = o, e, \tag{A13}$$

and since, by (A11) and (A12), $\zeta^{-\alpha_1}\tilde{b}_p \to 0$ for $\zeta \to 0$, we have

$$K_p = \Re(k_p), \quad \text{where} \quad k_p = \int_0^{\infty} \frac{d}{d\zeta}(\zeta^{-\alpha_1} B_p)d\zeta\,. \tag{A14}$$

The evaluation of L_p follows similar lines, but is more complicated since the largest (K) terms must first be removed from (A11) and (A12) by differentiation. In this context it may be noted that the K and L terms shown are only the dominant terms of asymptotic expansions. For example, the $K_o\zeta^{\alpha_1}$ term in (A11) is the first term of an asymptotic expansion for $\zeta \to \infty$ the next term of which is $O(\zeta^{\alpha_1-8})$. Such terms may not be removed by the differentiation in (A15) below but they make no contribution to the limit

$$L_p = \frac{1}{\alpha_2 - \alpha_1} \mathrm{Lt}_{\zeta\to+\infty}\, \zeta^{1+\alpha_1-\alpha_2} \frac{d}{d\zeta}\left(\zeta^{-\alpha_1}\tilde{b}_p\right). \tag{A15}$$

We now have

$$L_p = \Re(\ell_p) \quad \text{where} \quad \ell_p = \frac{1}{\alpha_2-\alpha_1}\int_0^\infty \frac{d}{d\zeta}\left[\zeta^{1+\alpha_1-\alpha_2}\frac{d}{d\zeta}\left(\zeta^{-\alpha_1}B_p\right)\right] d\zeta\,. \tag{A16}$$

To evaluate k_o, ℓ_o, k_e and ℓ_e we follow the technique applied in Appendix A of Part 1. For example, we substitute (A11) into (A14) to obtain

$$k_o = 2^{-\frac{3}{2}\alpha_1}\,\mathcal{M}\left(P_o; \tfrac{1}{8}\alpha_2\right), \tag{A17}$$

where $\mathcal{M}$ denotes the Mellin transform and

$$P_o = \sum_{m=0}^{\infty} \frac{(-1)^m \gamma(2m+\alpha_1)\gamma(2m+8+\alpha_2)\mathrm{e}^{-i\pi m/4} z^{\frac{1}{4}m}}{\gamma(2m+1)\gamma(2m+5)\gamma(2m+6)\gamma(2m+8)\gamma(2m+10)\gamma(2m+11)}. \tag{A18}$$

The method of Appendix A of Part 1 then gives

$$\mathcal{M}(P_o;s) = \frac{4\pi e^{i\pi s}\,\mathrm{cosec}4\pi s\;\gamma(\alpha_1-8s)\,\gamma(8+\alpha_2-8s)}{\gamma(1-8s)\,\gamma(5-8s)\,\gamma(6-8s)\,\gamma(8-8s)\,\gamma(10-8s)\,\gamma(11-8s)}. \tag{A19}$$

By (A14) and (A17), we now have

$$K_o = \frac{4\pi\cos\frac{1}{8}\pi\alpha_2\,\mathrm{cosec}\frac{1}{2}\pi\alpha_2\,\gamma(\alpha_1-\alpha_2)}{2^{\frac{3}{2}\alpha_1}\gamma(1-\alpha_2)\gamma(5-\alpha_2)\gamma(6-\alpha_2)\gamma(8-\alpha_2)\gamma(10-\alpha_2)\gamma(11-\alpha_2)}, \tag{A20}$$

$$L_o = \frac{4\pi\cos\frac{1}{8}\pi\alpha_1\,\mathrm{cosec}\frac{1}{2}\pi\alpha_1\,\gamma(\alpha_2-\alpha_1)}{2^{\frac{3}{2}\alpha_2}\gamma(1-\alpha_1)\gamma(5-\alpha_1)\gamma(6-\alpha_1)\gamma(8-\alpha_1)\gamma(10-\alpha_1)\gamma(11-\alpha_1)}, \tag{A21}$$

$$K_e = -\frac{4\pi\cos\frac{1}{8}\pi\alpha_1\,\mathrm{cosec}\frac{1}{2}\pi\alpha_1\,\gamma(\alpha_1-\alpha_2)}{2^{\frac{3}{2}\alpha_1}\gamma(1-\alpha_2)\gamma(5-\alpha_2)\gamma(6-\alpha_2)\gamma(8-\alpha_2)\gamma(10-\alpha_2)\gamma(11-\alpha_2)}, \tag{A22}$$

$$L_e = -\frac{4\pi\cos\frac{1}{8}\pi\alpha_2\,\mathrm{cosec}\frac{1}{2}\pi\alpha_2\,\gamma(\alpha_2-\alpha_1)}{2^{\frac{3}{2}\alpha_2}\gamma(1-\alpha_1)\gamma(5-\alpha_1)\gamma(6-\alpha_1)\gamma(8-\alpha_1)\gamma(10-\alpha_1)\gamma(11-\alpha_1)}, \tag{A23}$$

the last three following by repetitions of the same argument. By (A20) – (A23) we have

$$\frac{L_o}{K_o} = \xi Q\,, \qquad \frac{L_e}{K_e} = \xi^{-1}Q\,, \tag{A24}$$

where

$$\xi = \frac{\cos\frac{1}{8}\pi\alpha_1 \ \sin\frac{1}{2}\pi\alpha_2}{\cos\frac{1}{8}\pi\alpha_2 \ \sin\frac{1}{2}\pi\alpha_1}, \tag{A25}$$

$$Q = 2^{\frac{3}{2}(\alpha_1-\alpha_2)}\frac{\gamma(1-\alpha_2)\gamma(5-\alpha_2)\gamma(6-\alpha_2)\gamma(8-\alpha_2)\gamma(10-\alpha_2)\gamma(11-\alpha_2)\gamma(\alpha_2-\alpha_1)}{\gamma(1-\alpha_1)\gamma(5-\alpha_1)\gamma(6-\alpha_1)\gamma(8-\alpha_1)\gamma(10-\alpha_1)\gamma(11-\alpha_1)\gamma(\alpha_1-\alpha_2)}. \tag{A26}$$

We are particularly interested in these results for $\widehat{r}_m \ll 1$, when $\alpha_1 \doteq 2-\widehat{r}_m$, $\alpha_2 \doteq 1+\widehat{r}_m$. Then, by (A25) and (A26),

$$\xi \doteq \frac{2^{5/4}}{\widehat{r}_m\,\pi(1+\sqrt{2})^{1/2}} \doteq \frac{0.4872476}{\widehat{r}_m}, \tag{A27}$$

$$Q \doteq -\frac{4\sqrt{2}\,\Gamma\left(\frac{5}{8}\right)\Gamma\left(\frac{7}{8}\right)\Gamma\left(\frac{1}{4}\right)}{\widehat{r}_m\,\Gamma\left(\frac{1}{8}\right)\Gamma\left(\frac{3}{8}\right)\Gamma\left(\frac{3}{4}\right)} \doteq -\frac{1.4649270}{\widehat{r}_m}, \tag{A28}$$

and (A24) becomes

$$\frac{L_o}{K_o} \doteq -\frac{0.7137821}{\widehat{r}_m^2}, \qquad \frac{L_e}{K_e} \doteq -3.006535\,. \tag{A29}$$

When $\widehat{r} < 0$, the terms of (A3) are no longer in descending order of magnitude for $|\zeta| \to \infty$, since then $|\zeta| \gg |\zeta|^{\alpha_2}$. The argument just presented can, however, be modified. In place of (A15), we use

$$L_p = \frac{1}{(\alpha_2-1)(\alpha_2-\alpha_1)}\,\mathrm{Lt}_{\zeta\to+\infty}\,\zeta^{2-\alpha_2}\frac{d}{d\zeta}\left[\zeta^{\alpha_1}\frac{d}{d\zeta}\left(\zeta^{-\alpha_1}\tilde{b}_p\right)\right]. \tag{A30}$$

An analysis too similar to the one just presented to be repeated here again leads to (A21) and (A23). In other words, (A20) – (A29) remain valid not just for $0 < \widehat{r}_m < \frac{1}{4}$ but for $|\widehat{r}_m| < \frac{1}{4}$.

Since (A2) are themselves solutions of the critical layer equation, we obtain two new solutions b_e and b_e by subtracting $M_o\zeta$ and M_e from $\tilde{b}_o$ and $\tilde{b}_e$ respectively. By (A3) and (A4), these are such that

$$b_o \sim (K_o|\zeta|^{\alpha_1} + L_o|\zeta|^{\alpha_2})\ \mathrm{sgn}\ \zeta\,, \qquad \zeta \to \pm\infty\,, \tag{A31}$$

$$b_e \sim K_e|\zeta|^{\alpha_1} + L_e|\zeta|^{\alpha_2}, \qquad \zeta \to \pm\infty\,, \tag{A32}$$

apart from exponentially small terms. It is these functions that we employ in §3.

Finally, we note that the constant appearing in the second of (A29) coincides with the constant $-A_p$ used in Part 1 and derived there by a different asymptotic argument. To establish the connection, we need to include the first correction to the inner solution b_1:

$$b_1 \ = \ 1 \ + \ \tfrac{1}{2}(s\Lambda + k^2)\delta^2\zeta^2. \tag{A33}$$

Within the critical layer, the tearing mode is dominantly even, so that (apart from an inconsequential term proportional to b_2)

$$b_z \sim K_e\zeta^2 + L_e|\zeta| + b_{zc}[1 + \tfrac{1}{2}(s\Lambda + k^2)\delta^2\zeta^2], \qquad |\zeta| \to \infty, \tag{A34}$$

which implies that the outer solution has the form

$$b_z \sim b_{zc} + L_e|z - z_c| + \left[\tfrac{1}{2}(s\Lambda + k^2)b_{zc} + \frac{K_e}{\delta^2}\right](z - z_c)^2, \qquad |z - z_c| \to 0. \tag{A35}$$

It follows that

$$(db_z/dz)_{z_c+} = -(db_z/dz)_{z_c-} = L_e/\delta, \tag{A36}$$

$$(d^2b_z/dz^2)_c = (s\Lambda + k^2)b_{zc} + 2K_e/\delta^2. \tag{A37}$$

Now according to (3.1), the outer solution obeys

$$\frac{d^2b_z}{dz^2} = \left(k^2 + \frac{1}{F}\frac{d^2F}{dz^2}\right)b_z, \tag{A38}$$

and it therefore follows from (A37) that

$$\left[s\Lambda - \frac{1}{F}\frac{d^2F}{dz^2}\right]b_{zc} = -\frac{2K_e}{\delta^2}. \tag{A39}$$

From (A36) it is now clear that $\Lambda s = O(\delta^{-1})$ so that (A39) simplifies to

$$b_{zc} = -2K_e/\delta^2\Lambda s, \tag{A39}$$

and by (A36) we finally obtain

$$\Delta \equiv \left[\frac{1}{b_z}\frac{db_z}{dz}\right]_{z_c-}^{z_c+} = A_p\delta\Lambda s, \tag{A40}$$

which agrees with (3.19) in Part 1.

Appendix B. Asymptotics of steady convection in a non-rotating layer

The classic paper of Furth *et al.* (1963) describes very completely the tearing and g-modes of a non-rotating plasma. The convective modes were less fully investigated, and are studied here. The Lundquist number S, defined by

$$S = \frac{\tau_\eta}{\tau_H}, \qquad \tau_\eta = \frac{d^2}{\eta}, \qquad \tau_H = \frac{d}{V_A}, \qquad V_A = \frac{B_0}{\sqrt{(\mu_0\rho_0)}}, \tag{B1}$$

plays a role analogous to the Elsasser number for the rotating layer. Equations (2.2) – (2.5) hold as before, but (2.1) is replaced (in the Boussinesq approximation) by

$$\rho_0(\partial_t + \mathbf{V}\cdot\nabla)\mathbf{V} = -\nabla P + \mathbf{J}\times\mathbf{B} + \rho_0 C\mathbf{g} + \rho_0\nu\nabla^2\mathbf{V}, \tag{B2}$$

where ν is the kinematic viscosity.

We make the substitutions (2.6) – (2.8) and use dimensionless variables based on d as unit of length and τ_H as unit of time. Equations (2.9) – (2.13) are replaced by

$$v_z = \frac{i}{F}\left\{\frac{1}{S}(D^2 - k^2) - s\right\}b_z, \tag{B3}$$

$$\omega_z = \frac{i}{F}\left\{\frac{1}{S}(D^2 - k^2) - s\right\}j_z - \frac{\bar{F}}{F}v_z, \tag{B4}$$

$$j_z = \frac{i}{F}\left\{\frac{p_m}{S}(D^2 - k^2) - s\right\}\omega_z + \frac{\bar{F}}{F}b_z, \tag{B5}$$

$$(D^2 - k^2)\left\{\frac{p_m}{S}(D^2 - k^2) - s\right\}v_z + i\left[F(D^2 - k^2) - D^2F\right]b_z - Rk^2c = 0, \tag{B6}$$

$$v_z = -\left\{\frac{p_\kappa}{S}(D^2 - k^2) - s\right\}c, \tag{B7}$$

where $p_m = \nu/\eta$ is the magnetic Prandtl number. When $p_m \neq 0$, the boundary conditions (2.15) must be supplemented by noslip or stress-free conditions; we select the latter for definiteness, so obtaining

$$v_z = D^2v_z = b_z = c = 0, \qquad \text{at} \quad z = 0, 1, \tag{B8}$$

$$D\omega_z = Dj_z = 0, \qquad \text{at} \quad z = 0, 1. \tag{B9}$$

The system (B3) – (B9) factorizes into two distinct subsystems. Equations (B3) and (B6) – (B8) define an eigenvalue problem for s, v_z, b_z and c. Once a nontrivial solution has been found, (B4), (B5) and (B9) may, if desired, be solved to determine the corresponding ω_z and j_z. We shall ignore this aspect of the problem; we are interested primarily in finding s, and shall therefore focus on (B3) and (B6) – (B8) alone. More precisely, we wish to find conditions for the onset of steady convection, i.e. values of R for which $s = 0$ is an eigenvalue. We are therefore interested in nontrivial solutions of

$$(D^2 - k^2)\left\{\frac{p_m}{S^2}(D^2 - k^2)^2\frac{1}{F}(D^2 - k^2) + F(D^2 - k^2) - D^2F\right\}b_z + \frac{R_mk^2}{p_\kappa F}(D^2 - k^2)b_z = 0, \tag{B10}$$

subject to the boundary conditions (B8) which require that

$$b_z = D^2b_z = 0, \qquad \text{at} \quad z = 0, 1, \tag{B11}$$

together with two further conditions at each boundary that involve higher derivatives of b_z.

In the limit $S \to \infty$, the solution of (B10) consists of outer regions in which (3.1) – (3.5) hold as before, passive boundary layers at $z = 0$, and 1, which adjust the outer solutions to the higher order conditions referred to below (B11), and critical layers surrounding critical levels at which $F = 0$. To leading order, it is necessary only that the outer solutions satisfy (B11).

The structure of the critical layers differs from that analyzed in Appendix A. Their thickness is of order

$$\delta = \frac{p_m^{1/6}}{S^{1/3}|F_c'|^{1/3}}, \tag{B12}$$

an equation that replaces (3.6). Using this δ in the definition (3.7) of the stretched coordinate ζ, we obtain in place of (3.8) the critical layer equation

$$[D^2(D^4 + \zeta^2) + \widehat{r}_m]\left(\frac{1}{\zeta}D^2 b_z\right) = 0. \tag{B13}$$

The analysis of (B13) is too similar to that set out in Appendix A to be repeated here. Suffice it to say that solutions odd and even in ζ again exist for which (3.13), (3.14) and (A24) hold; (A25) and (A26) are replaced by

$$\xi = \frac{\sin\frac{1}{2}\pi\alpha_2}{\sin\frac{1}{2}\pi\alpha_1}, \tag{B14}$$

$$Q = 6^{\frac{2}{3}(\alpha_1-\alpha_2)}\frac{\widehat{\gamma}(1-\alpha_2)\widehat{\gamma}(4-\alpha_2)\widehat{\gamma}(5-\alpha_2)\widehat{\gamma}(6-\alpha_2)\widehat{\gamma}(8-\alpha_2)\widehat{\gamma}(9-\alpha_2)\widehat{\gamma}(\alpha_2-\alpha_1)}{\widehat{\gamma}(1-\alpha_1)\widehat{\gamma}(4-\alpha_1)\widehat{\gamma}(5-\alpha_1)\widehat{\gamma}(6-\alpha_1)\widehat{\gamma}(8-\alpha_1)\widehat{\gamma}(9-\alpha_1)\widehat{\gamma}(\alpha_1-\alpha_2)}, \tag{B15}$$

where $\widehat{\gamma}(x) = \Gamma(\frac{1}{6}x)$. When $\widehat{r}_m \ll 1$, these reduce to

$$\xi \approx \frac{2}{\pi\widehat{r}_m} \approx \frac{0.6366197}{\widehat{r}_m}, \tag{B16}$$

$$Q \approx -\left(\frac{4}{3}\right)^{1/3}\frac{1}{\widehat{r}_m} \approx -\frac{1.1006424}{\widehat{r}_m}. \tag{B17}$$

The argument given below (3.17) holds with minor modifications, and we again find that, in the marginal state, $\widehat{r}_m = O(\delta)$, i.e. $\widehat{r}_m = O(S^{-1/3})$; cf. (3.19).

In place of (3.28), we now have

$$\widehat{r}_m \sim \frac{0.2131384p_m^{1/6}}{|F_c'|^{1/3}}\frac{k\sinh k}{\sinh kz_c\sinh k(1-z_c)}S^{-1/3}, \qquad S \to \infty. \tag{B18}$$

The minimum $\widehat{r}_m$ as a function of z_c occurs as before when $z_c = \frac{1}{2}$, and the resulting $\widehat{r}_m$ has a single minimum at $k \approx 1.6221312$ for which

$$\widehat{r}_c \sim \frac{0.8781305p_m^{1/6}}{|F_c'/k|^{1/3}}S^{-1/3}, \qquad S \to \infty. \tag{B19}$$

Figure 12, which shows $R_m(S)/p_\kappa$ for model (B1) with $p_m = 1$, $q = \frac{3}{2}\pi$ and $k_x = k_y = 4$, was obtained by integrating the full equations. The asymptote (B18) is also shown. The agreement is very satisfactory.

LEGENDS FOR FIGURES

Figure 1. The critical direct mode for $q = \frac{3}{2}\pi$. In (a) $-R_c/p_\kappa$ is shown as a function of Λ; (b) shows the corresponding value of k_c; and (c) shows the location of one of the critical levels $z = z_2$. (The other critical level is situated at $z = z_1 \equiv z_2 - \frac{2}{3}$.)

Figure 2. Variation of R_m/p_κ with k_y/k for $k = 4\sqrt{2}$ and $k_x > 0$ illustrating how the direction of $\mathbf{k}$ affects the ease with which convection occurs; $q = \frac{3}{2}\pi$ and $\Lambda = 10^6$. The mode most easily excited ($k_x = k_y = 4$) has one critical layer situated centrally at $z_c = \frac{1}{2}$; the hardest mode to excite ($k_x = -k_y = 4$) has two critical modes, situated symmetrically at $z_1 = \frac{1}{6}$ and $z_2 = \frac{5}{6}$.

Figure 3. Variation of R_m/p_κ with Λ for direct modes when $k = 4\sqrt{2}$. The dashed curve shows the case $k_x = k_y = 4$ of one centrally placed critical layer; the full line exhibits the corresponding asymptotic result ($R_m/p_\kappa \sim 8.74418\Lambda^{-1/4}$) given by (3.28). The dashed and dotted curve shows the case $k_x = -k_y = 4$ of two symmetrically placed critical layers.

Figure 4. Eigenfunctions (a) v_z; (b) b_z; (c) c for $\Lambda = 10^6$ and $q = \frac{3}{2}\pi$ and for the marginal direct mode with $k_x = k_y = 4$ (a case of one critical level); (d), (e) and (f) show the same functions for the corresponding case $k_x = -k_y = 4$ of two critical levels.

Figure 5. Variation of R_m/p_κ with Λ for $q = \frac{1}{2}\pi$. The dashed curve shows the case $k_x = -k_y = \frac{1}{2}$ of one centrally placed critical layer; the full line exhibits the corresponding asymptotic result ($R_m/p_\kappa \sim 1.74016\Lambda^{-1/4}$) given by (3.28).

Figure 6. Variation of $-R_m/p_\kappa$ with Λ for $k = \sqrt{2}$ and $q = \frac{3}{2}\pi$. The solid curve shows the case $k_x = k_y = 1$ of one centrally placed critical layer. The dashed curve shows the case $k_x = -k_y = 1$ of two symmetrically placed critical layers.

Figure 7. Eigenfunctions (a) v_z; (b) b_z; (c) c for $\Lambda = 10^6$ and $q = \frac{3}{2}\pi$ and for $k_x = k_y = 1$ (a case of one critical level); (d), (e) and (f) show the same functions for the corresponding case $k_x = -k_y = 1$ of two critical levels.

Figure 8. Overstable modes for $p_\kappa = 5$ and $k_x = k_y = 4$ with $q = \frac{3}{2}\pi$. In (a) the marginal value of R_m/p_κ is shown as function of Λ; the corresponding R_m/p_κ for direct modes is given by the solid curve. In (b) the frequency, $\Im(s)$, is shown as a function of Λ.

Figure 9. Overstable modes for $p_\kappa = 10$ and $k_x = k_y = 4$ with $q = \frac{3}{2}\pi$. In (a) the marginal value of R_m/p_κ is shown as function of Λ; the corresponding R_m/p_κ for direct modes is given by the solid curve. In (b) the frequency, $\Im(s)$, is shown as a function of Λ.

Figure 10. Isolines of density perturbation, c, in tearing-type modes, shown across the entire layer in the plane perpendicular to $\mathbf{B}_0$ at the critical level. One horizontal wavelength is shown, for $\Lambda = 10^6$ and $q = \frac{3}{2}\pi$. In (a) $k_x = k_y = 1$, so that there is one critical layer at $z = \frac{1}{2}$; in (b), $k_x = -k_y = 1$, so that there are two critical layer at $z = \frac{1}{6}$ and $z = \frac{5}{6}$.

Figure 11. Isolines of density perturbation, c, in g-type modes, shown across the entire layer in the plane perpendicular to $\mathbf{B}_0$ at the critical level. One horizontal wavelength is shown, for $\Lambda = 10^6$ and $q = \frac{3}{2}\pi$. In (a) $k_x = k_y = 4$, so that there is one critical layer at $z = \frac{1}{2}$; in (b), $k_x = -k_y = 4$, so that there are two critical layer at $z = \frac{1}{6}$ and $z = \frac{5}{6}$.

Figure 12. Direct modes in the classical (non-rotating) case for $p_m = 1$, $q = \frac{3}{2}\pi$. The dashed line shows the value of R_m/p_κ obtained by numerical integration of (B3) and (B6)–(B8) as a function of S for $k_x = k_y = 4$, a case in which there is one centrally-located critical level; the full line is the corresponding asymptote $R_m/p_\kappa = 18.05142S^{-1/3}$ obtained from (B18). The dashed and dotted line is for $k_x = -k_y = 4$ in which there are two critical levels.

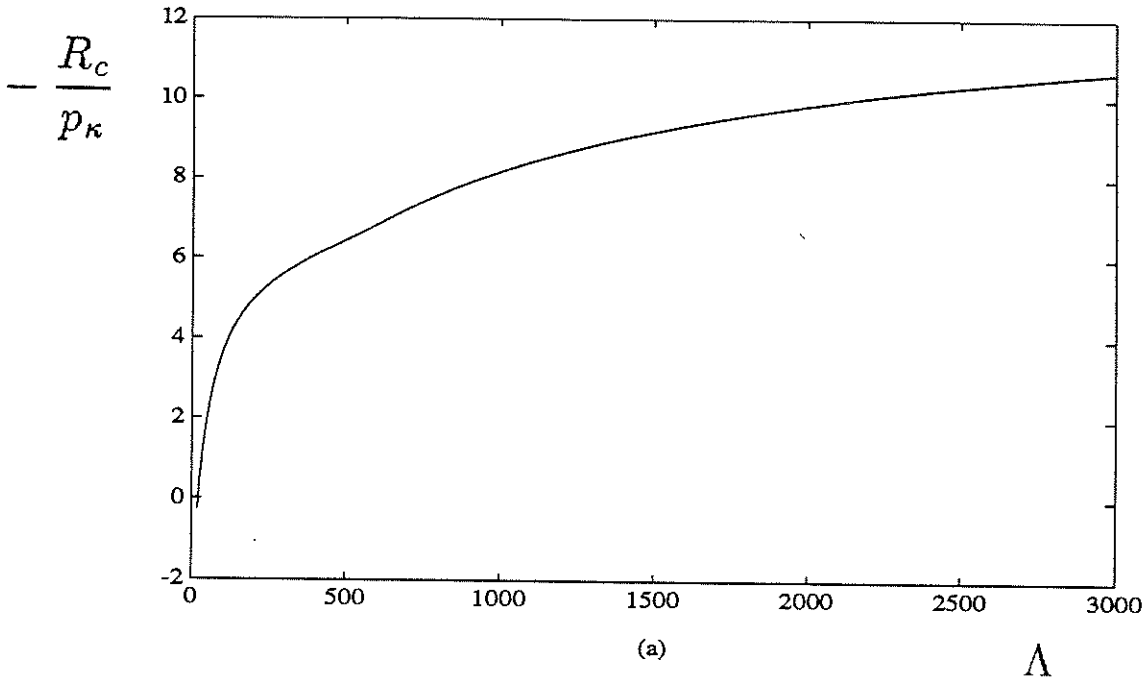
$-\frac{R_c}{p_\kappa}$
12
10
8
6
4
2
0
-2
0
500
1000
1500
2000
2500
3000
(a)
Λ

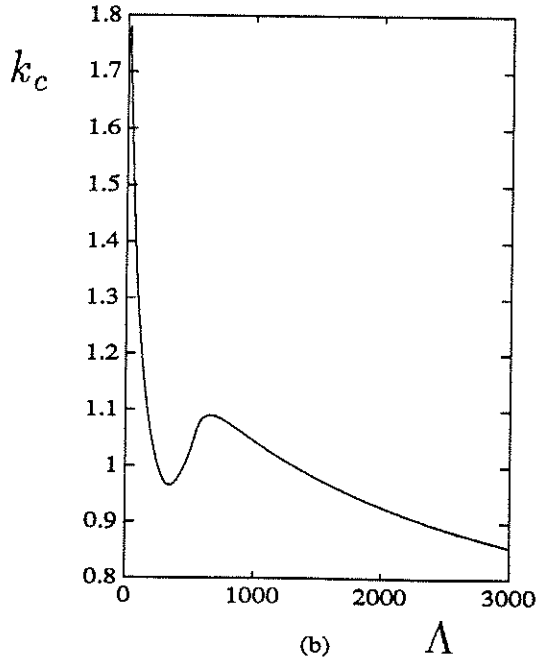
k_c
1.8
1.7
1.6
1.5
1.4
1.3
1.2
1.1
1
0.9
0.8
0
1000
2000
3000
(b)
Λ

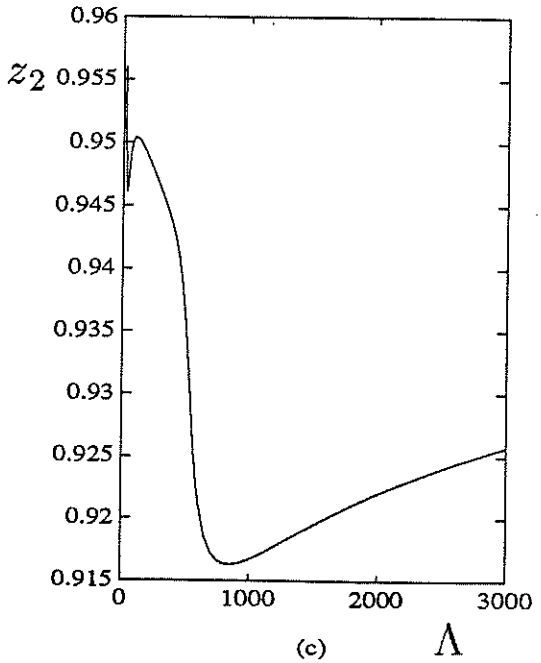
z_2
0.96
0.955
0.95
0.945
0.94
0.935
0.93
0.925
0.92
0.915
0
1000
2000
3000
(c)
Λ

Figures 1

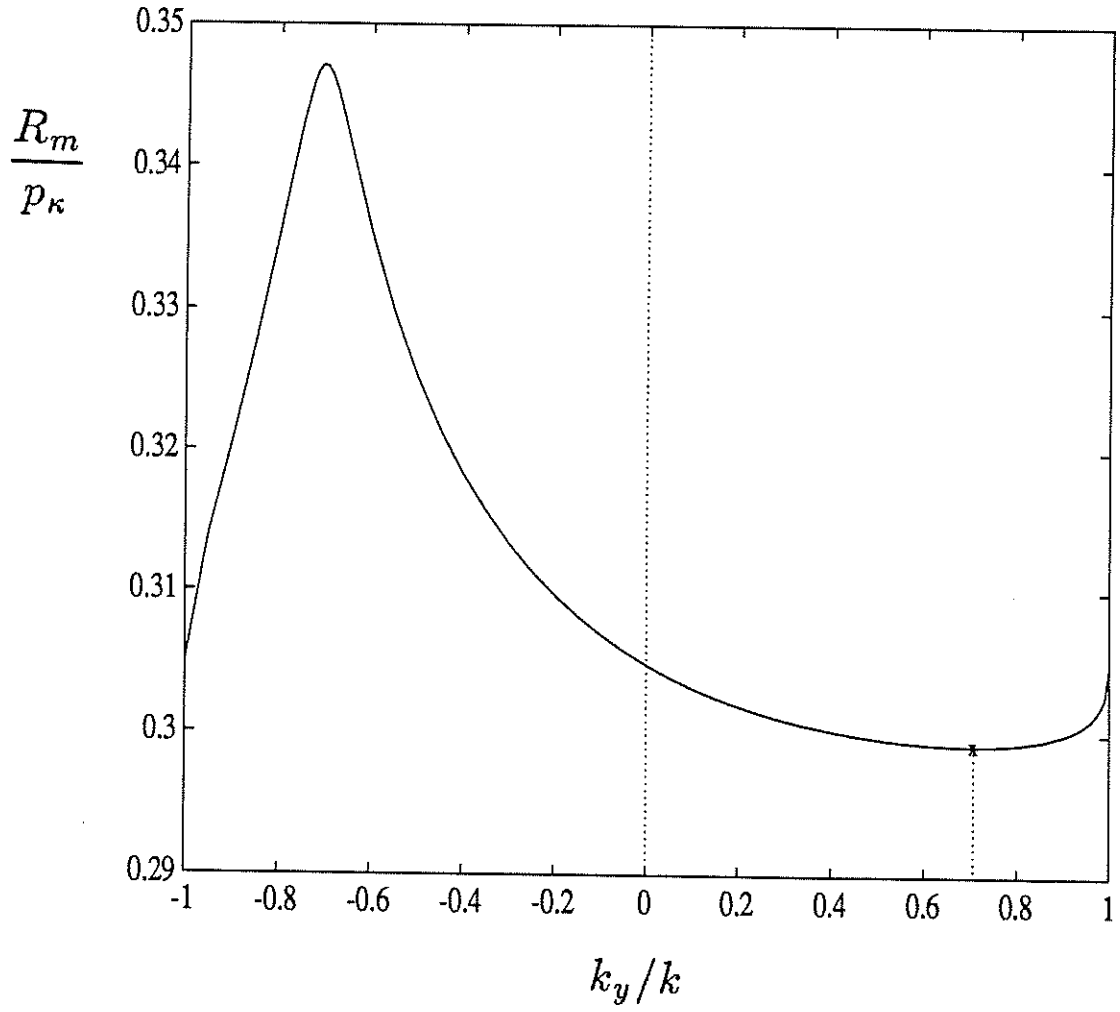
$\frac{R_m}{p_\kappa}$
0.35
0.34
0.33
0.32
0.31
0.3
0.29
-1
-0.8
-0.6
-0.4
-0.2
0
0.2
0.4
0.6
0.8
1
k_y/k

Figure 2

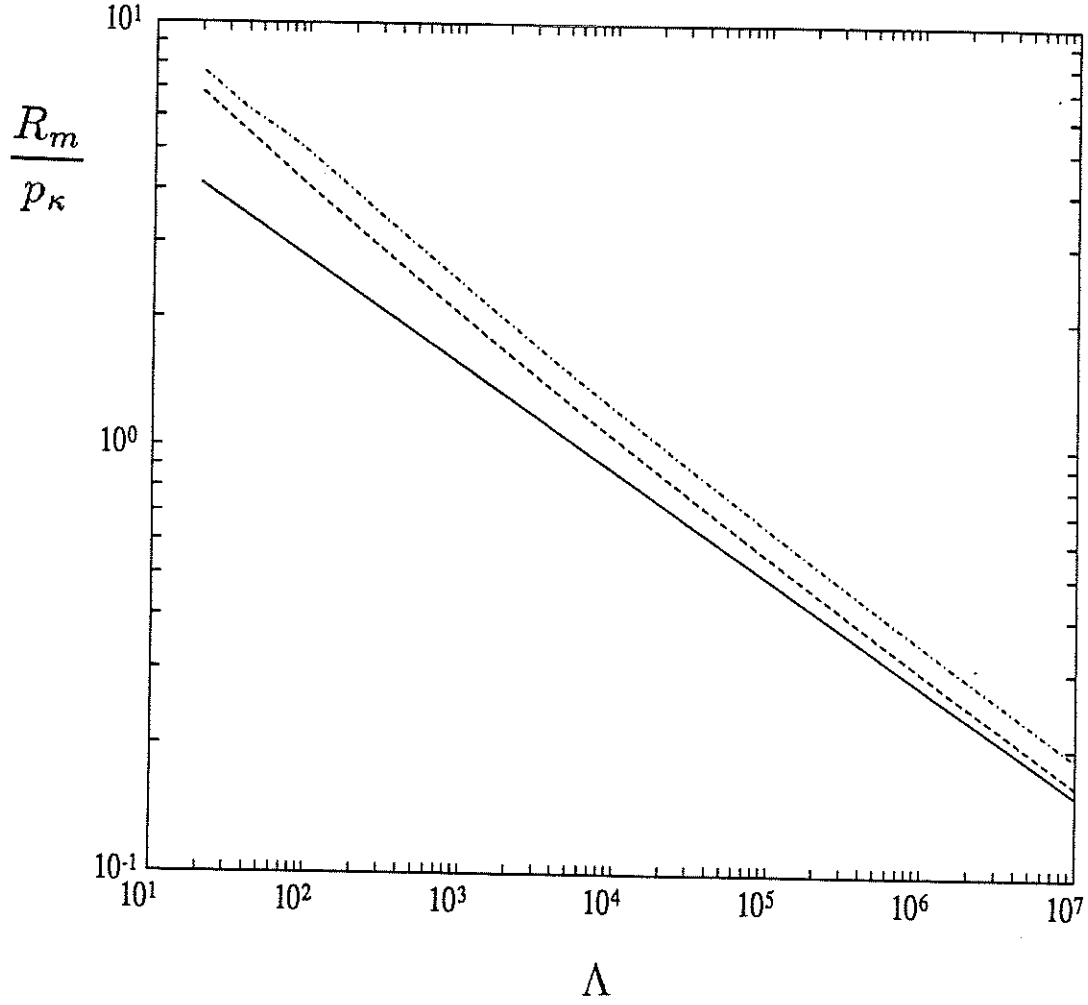

Figure 3

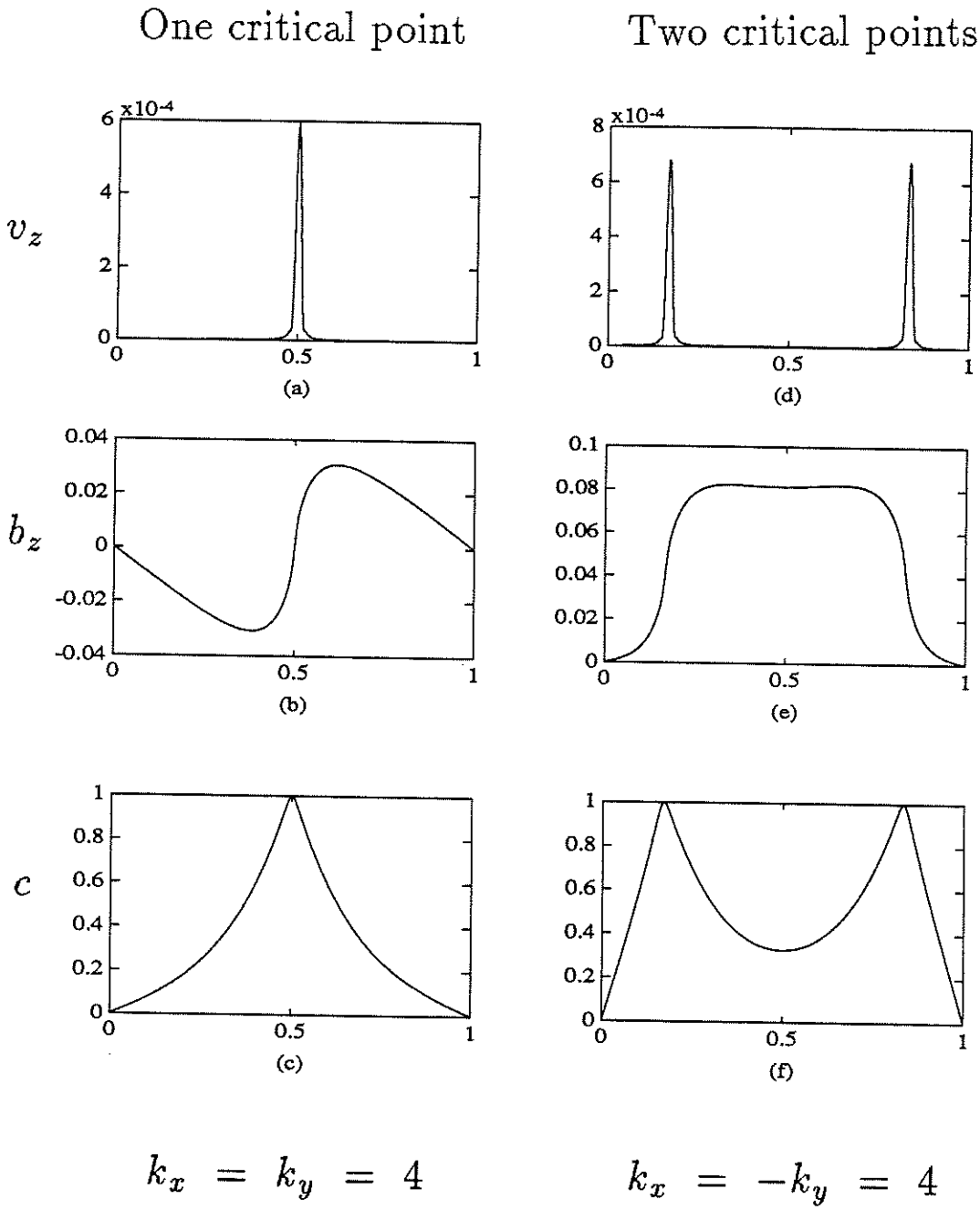
One critical point
Two critical points
v_z
b_z
c
x10-4
(a)
(b)
(c)
(d)
(e)
(f)
$k_x = k_y = 4$
$k_x = -k_y = 4$

Figures 4

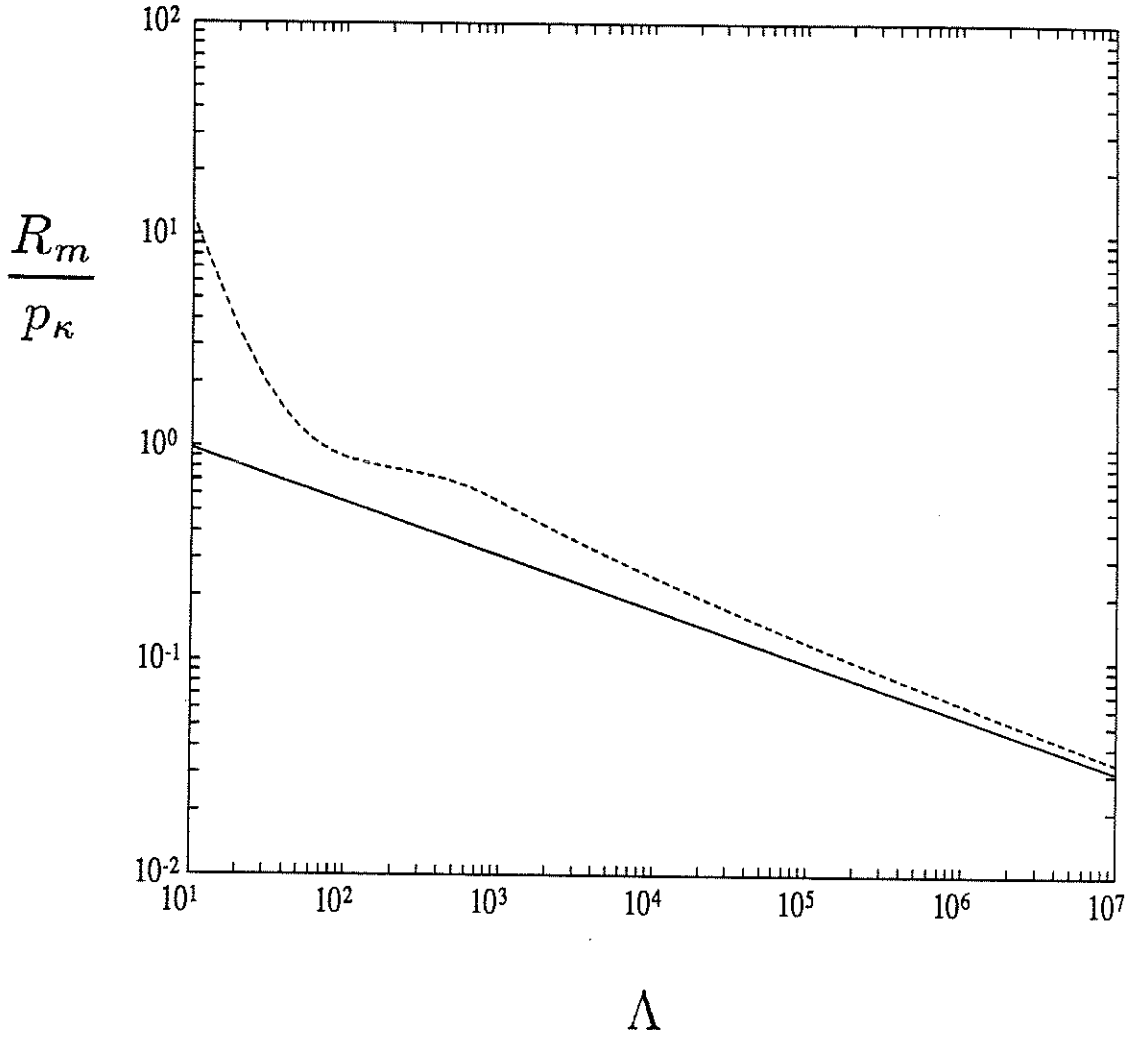
$\frac{R_m}{p_\kappa}$
10^2
10^1
10^0
10^{-1}
10^{-2}
10^1
10^2
10^3
10^4
10^5
10^6
10^7
Λ

Figure 5

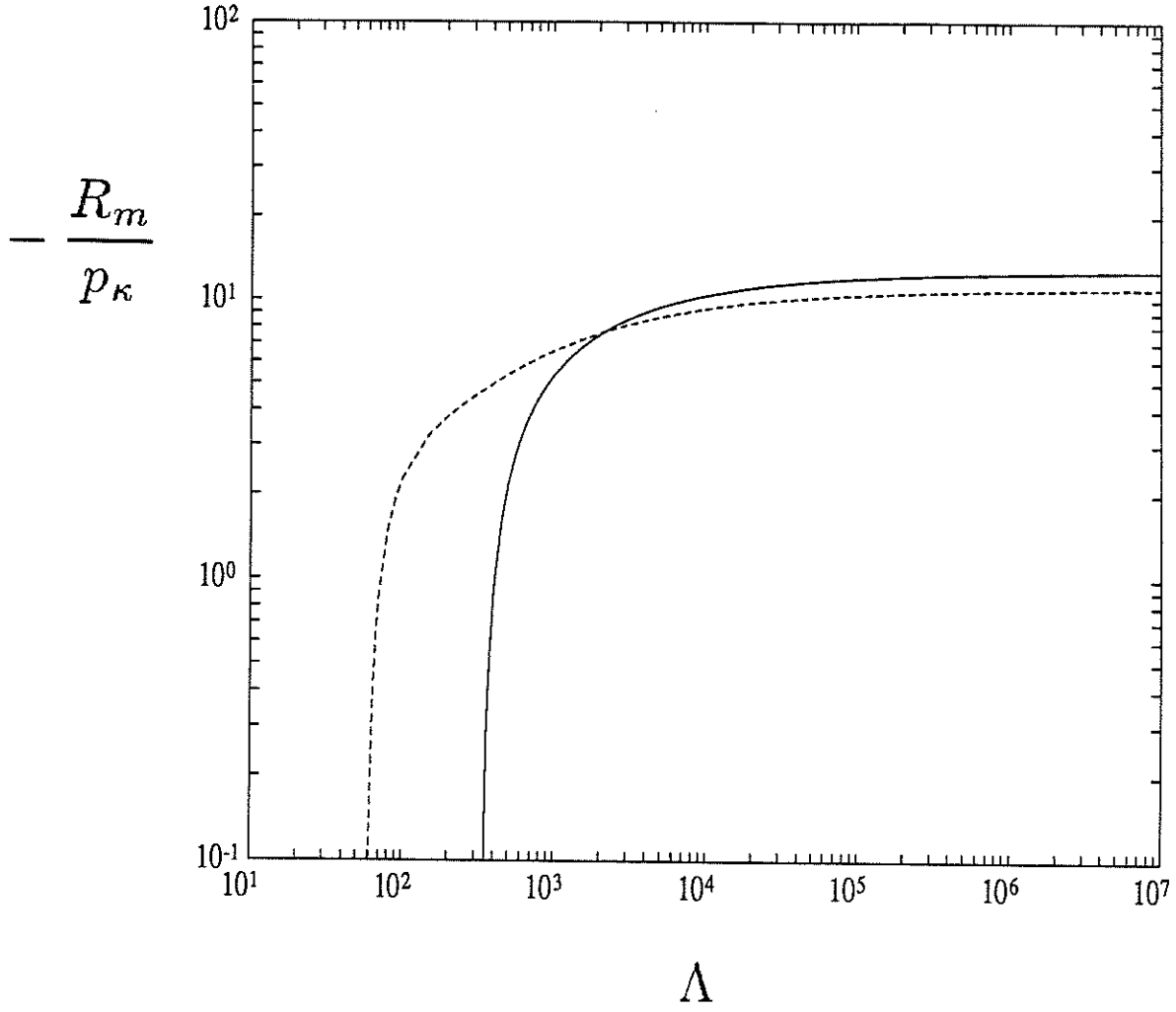
$-\frac{R_m}{p_\kappa}$
10^2
10^1
10^0
10^{-1}
10^1
10^2
10^3
10^4
10^5
10^6
10^7
Λ

Figure 6

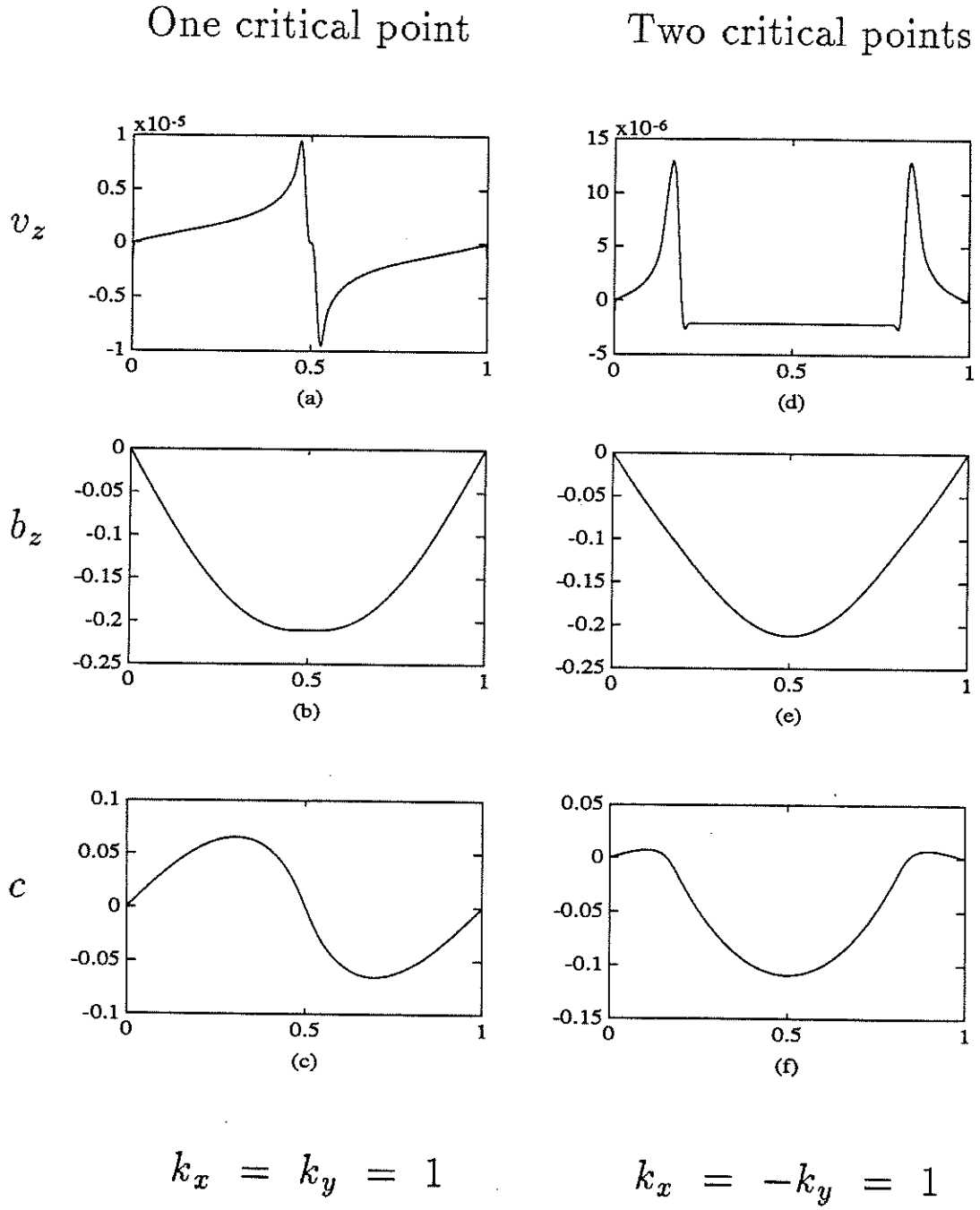
One critical point
Two critical points
v_z
b_z
c
x10-5
x10-6
(a)
(b)
(c)
(d)
(e)
(f)
$k_x = k_y = 1$
$k_x = -k_y = 1$

Figures 7

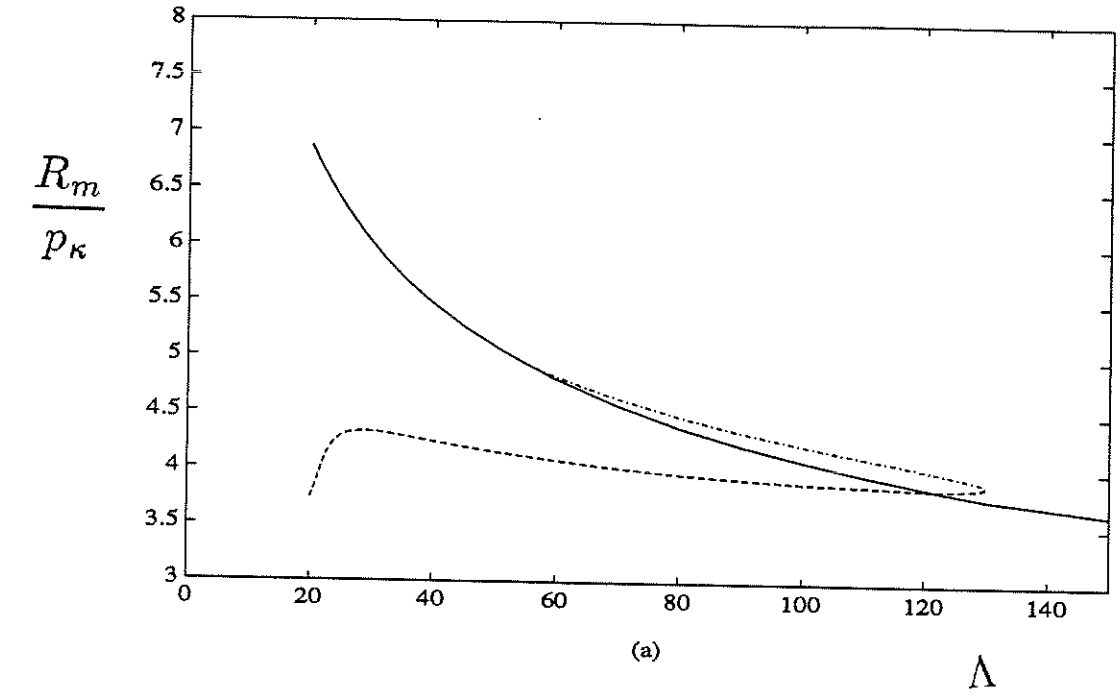
$\frac{R_m}{p_\kappa}$
8
7.5
7
6.5
6
5.5
5
4.5
4
3.5
3
0
20
40
60
80
100
120
140
(a)
Λ

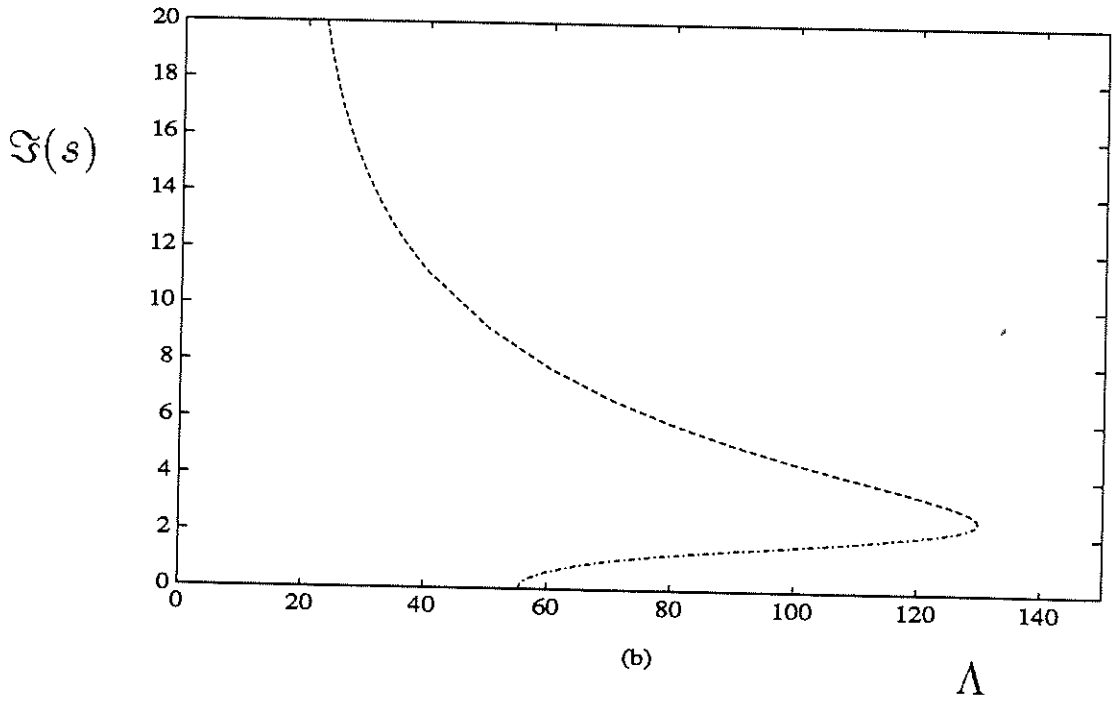
$\Im(s)$
20
18
16
14
12
10
8
6
4
2
0
0
20
40
60
80
100
120
140
(b)
Λ

Figures 8

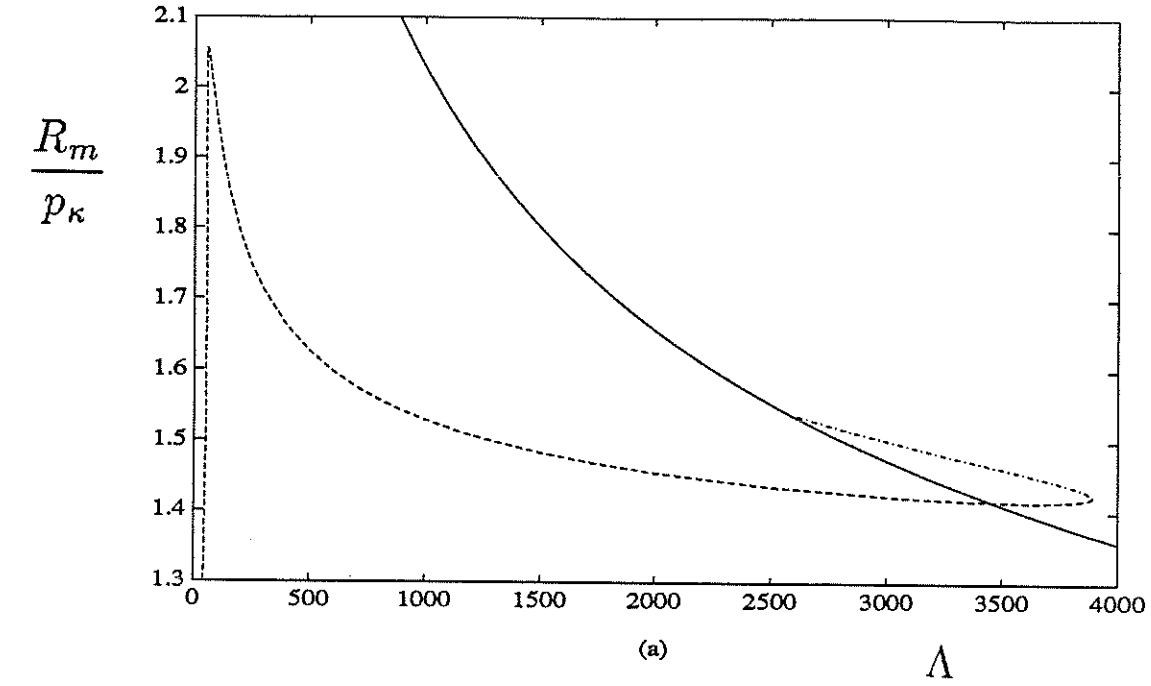
$\frac{R_m}{p_\kappa}$
2.1
2
1.9
1.8
1.7
1.6
1.5
1.4
1.3
0
500
1000
1500
2000
2500
3000
3500
4000
(a)
Λ

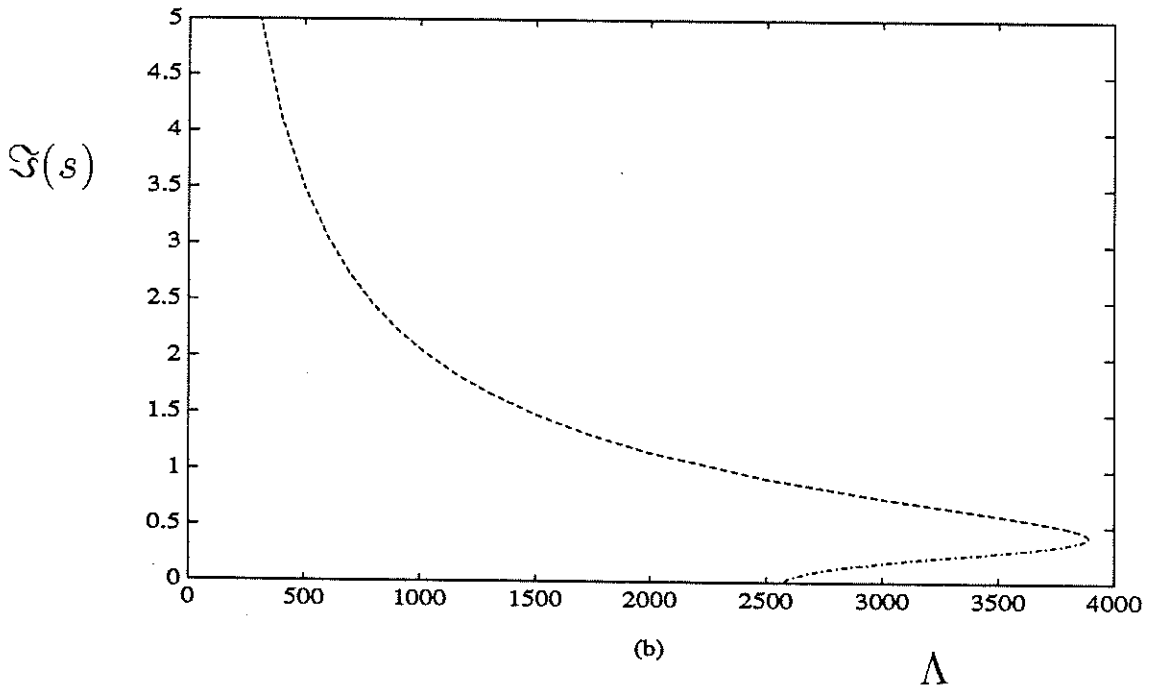
$\Im(s)$
5
4.5
4
3.5
3
2.5
2
1.5
1
0.5
0
0
500
1000
1500
2000
2500
3000
3500
4000
(b)
Λ

Figures 9

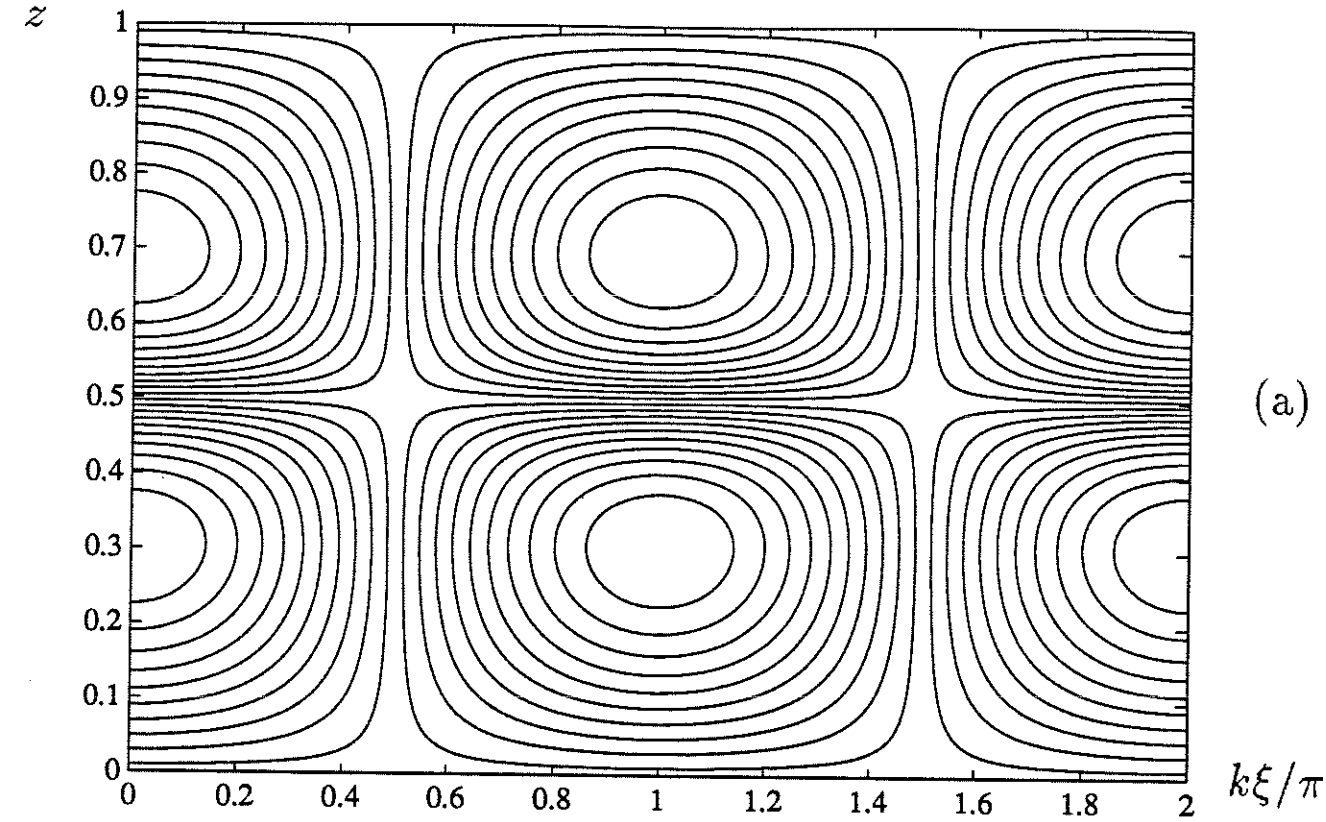
z
1
0.9
0.8
0.7
0.6
0.5
0.4
0.3
0.2
0.1
0
0
0.2
0.4
0.6
0.8
1
1.2
1.4
1.6
1.8
2
kξ/π
(a)

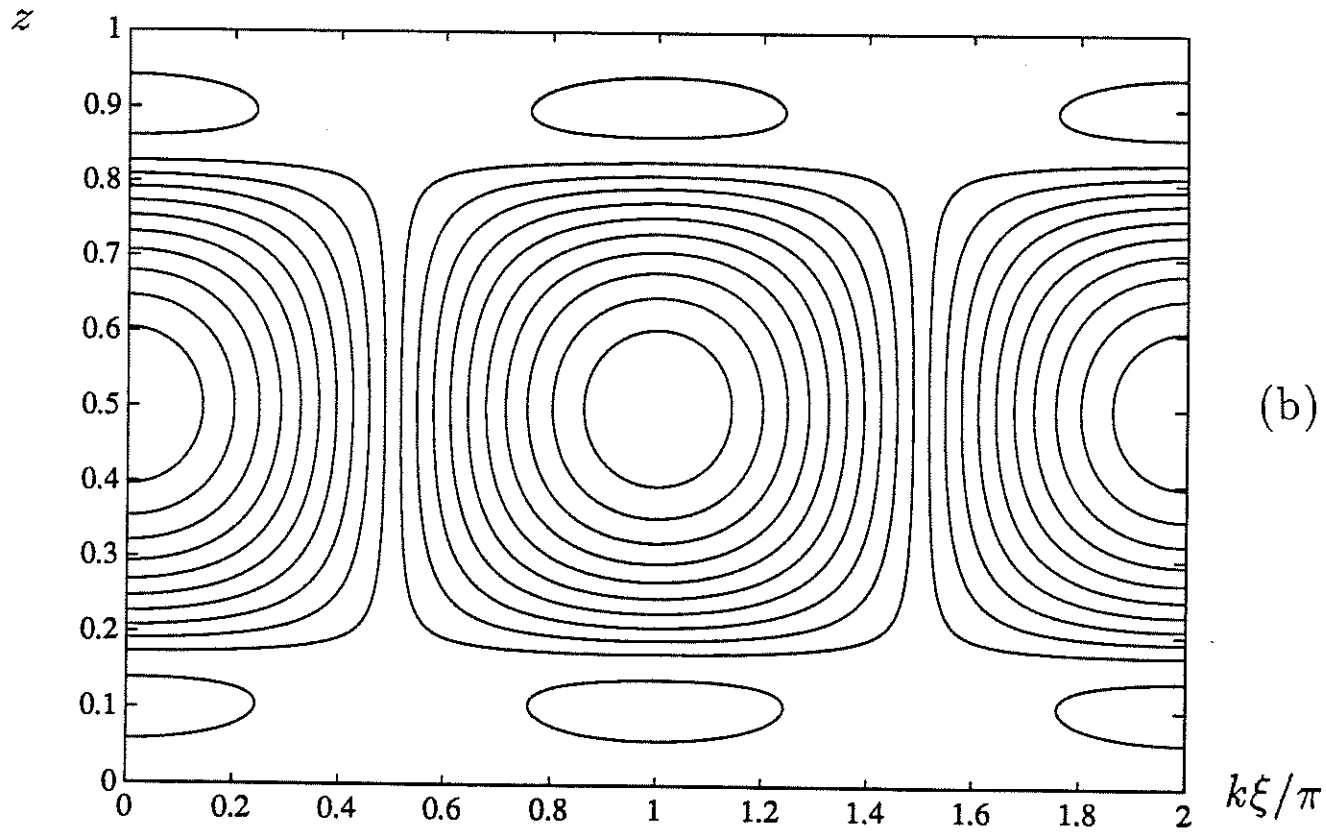
z
1
0.9
0.8
0.7
0.6
0.5
0.4
0.3
0.2
0.1
0
0
0.2
0.4
0.6
0.8
1
1.2
1.4
1.6
1.8
2
kξ/π
(b)

Figures 10

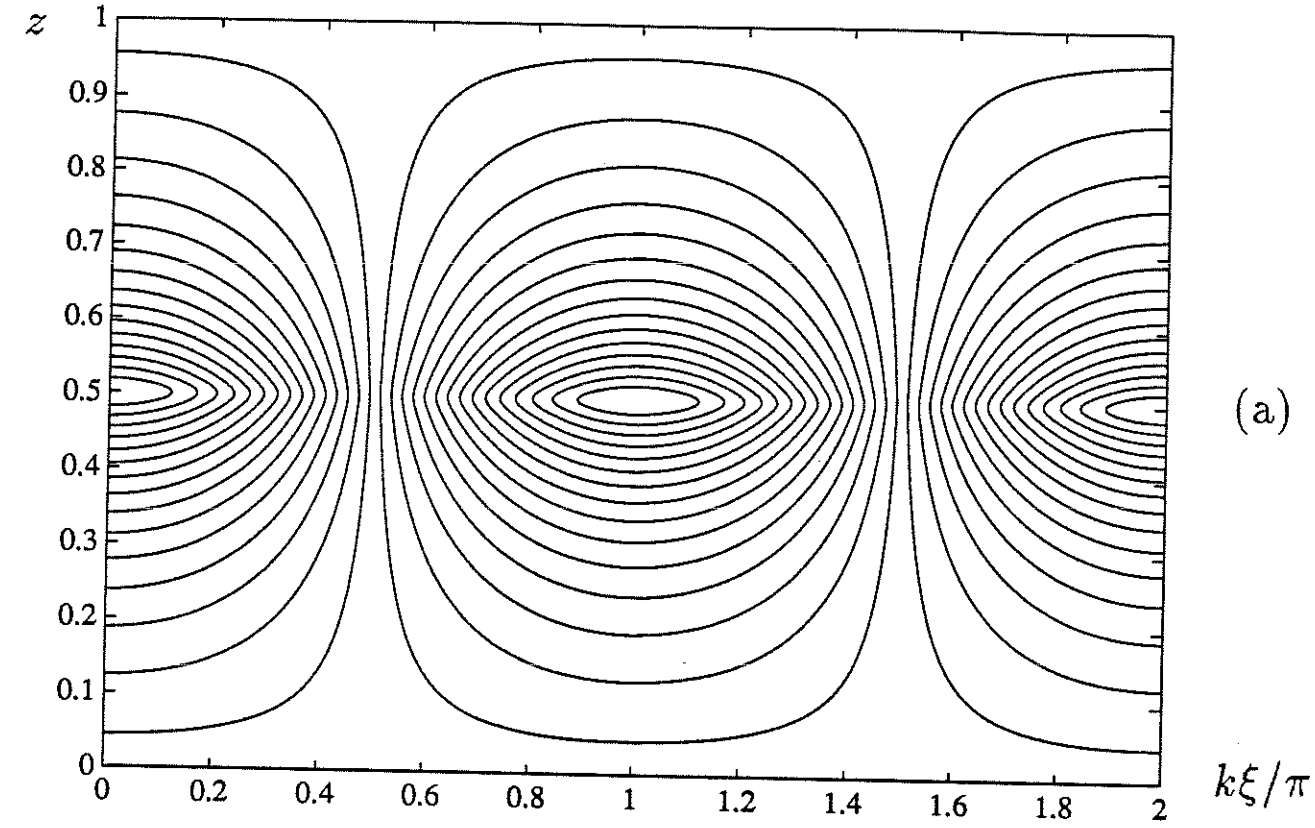

(a)

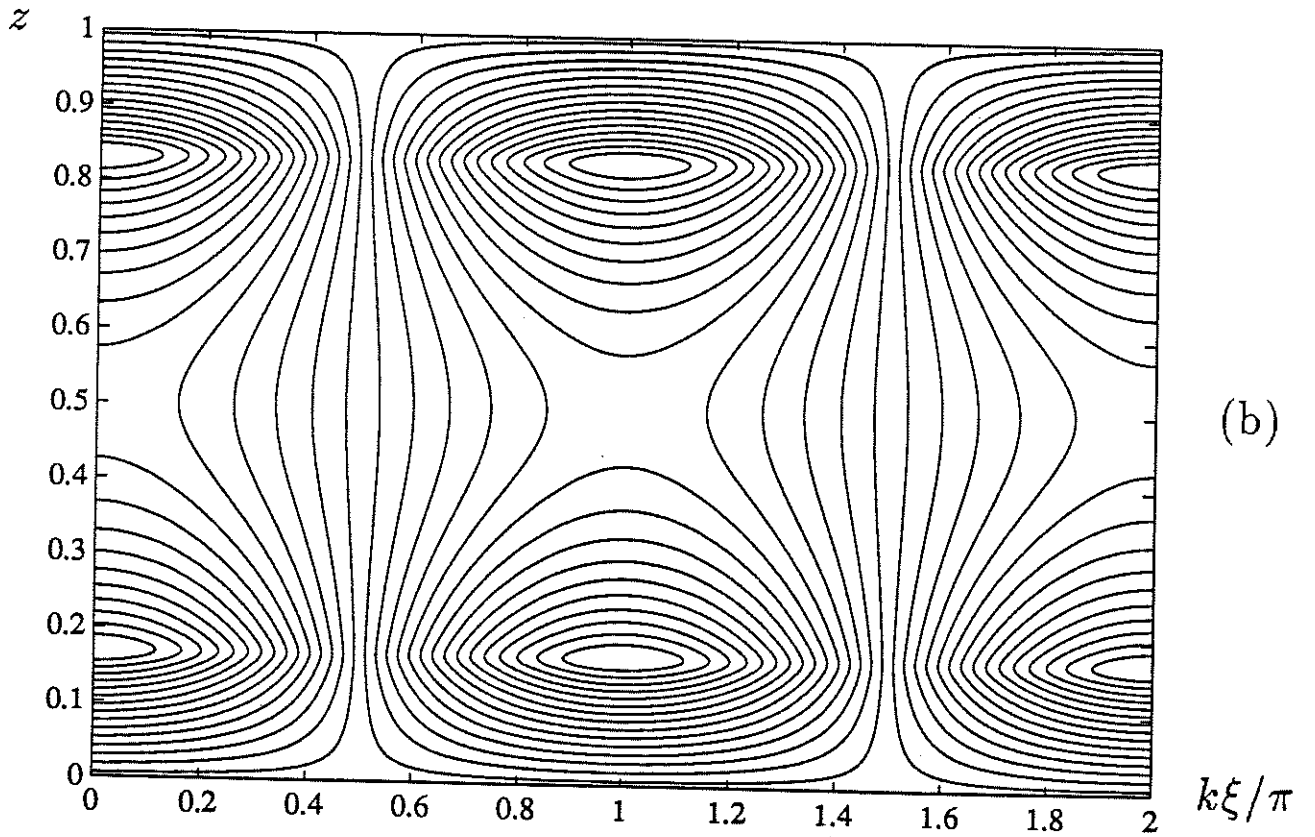

(b)

Figures 11

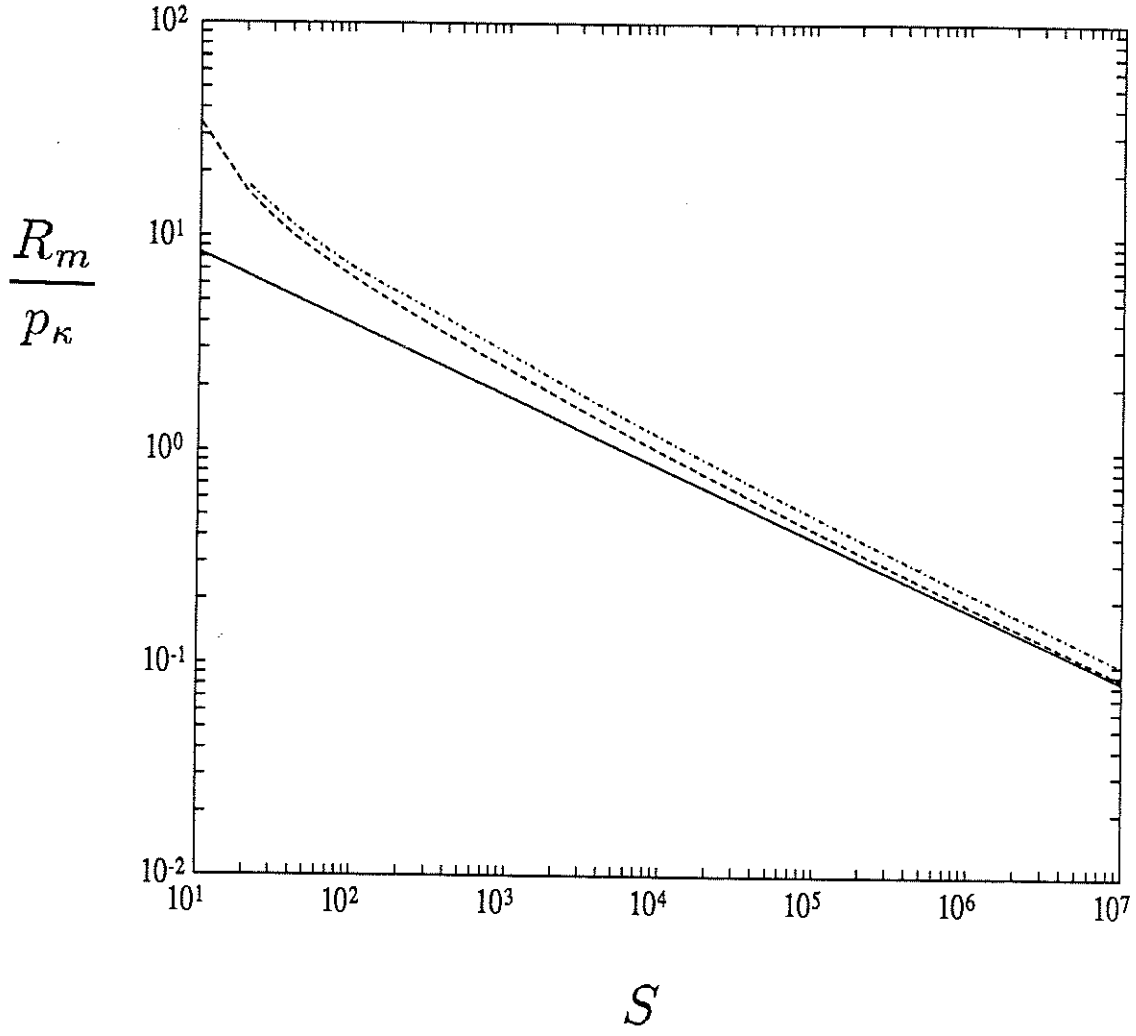

Figure 12